CHALMERS
UNIVERSITY OF TECHNOLOGY

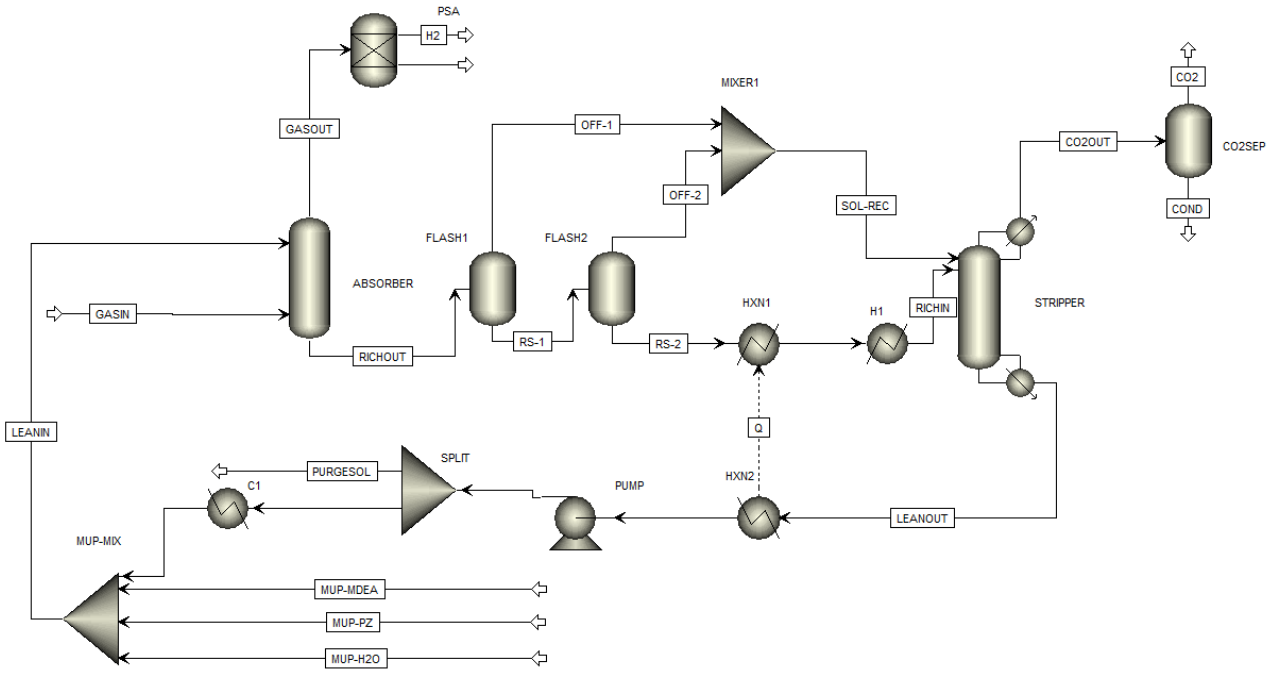

Evaluation of an Absorption Based aMDEA Process Using Aspen Plus

A conceptual study of biobased carbon capture technology for a combined heat and power plant

Master's thesis in Sustainable Energy Systems

JESPER LARSSON
TOVE LARSSON

DEPARTMENT OF SPACE, EARTH AND ENVIRONMENT
CHALMERS UNIVERSITY OF TECHNOLOGY
Gothenburg, Sweden 2022
www.chalmers.se

Master's thesis 2022

Evaluation of an Absorption Based aMDEA Process Using Aspen Plus

A conceptual study of biobased carbon capture technology for a combined heat and power plant

Jesper Larsson
Tove Larsson

CHALMERS
UNIVERSITY OF TECHNOLOGY

Department of Space, Earth and Environment
Division of Energy Technology
Chalmers University of Technology
Gothenburg, Sweden 2022

Evaluation of an Absorption Based aMDEA Process Using Aspen Plus
A conceptual study of biobased carbon capture technology for a combined heat and power plant
Jesper Larsson
Tove Larsson

Supervisor: Maja-Stina Svanberg Frisinger and Sima Ajdari, RISE
Examiner: Martin Seemann, Department of Space, Earth and Environment

Master's Thesis 2022
Department of Space, Earth and Environment
Division of Energy Technology
Chalmers University of Technology
SE-412 96 Gothenburg
Telephone +46 31 772 1000

Cover: A process flowsheet constructed in Aspen plus showing an absorption based carbon capture process.

Typeset in LaTeX
Printed by Chalmers Reproservice
Gothenburg, Sweden 2022

Evaluation of an Absorption Based aMDEA Process Using Aspen Plus
A conceptual study of biobased carbon capture technology for a combined heat and power plant

JESPER LARSSON
TOVE LARSSON
Department of Space, Earth and Environment
Chalmers University of Technology

Abstract

Production of heat and power through combustion of fossil fuels has contributed with increased levels of CO_2 in the atmosphere, causing climate change and environmental problems. A solution to contribute to a sustainable energy system and mitigate CO_2 emissions, is to combine biomass gasification with carbon capture technology. This thesis aims to investigate a hydrogen production unit for a combined heat and power plant, which includes chemical absorption based carbon capture. The solvent used is an aqueous solution of N-Methyldiethanolamine (MDEA) and piperazine (PZ).

Models for the hydrogen production process were constructed in the simulation software Aspen Plus. The carbon capture model was investigated in a parameter study where important process parameters were identified. Liquid-to-gas ratio, solvent composition, pressures levels in the absorption and desorption columns, and feed temperatures into the respective columns were investigated. An optimization with the objective of minimizing the heat demand in the process was also included in the model evaluation.

Liquid-to-gas ratio was found to have a large impact on the absorption efficiency, with increased absorption as a result of increased liquid-to-gas ratio. It was found that an optimum ratio could be located, where excess heating of the process was kept to a minimum. Investigation of solvent composition showed that the ratio between MDEA and PZ was a key design parameter, in terms of carbon capture efficiency and energy demand of the process. An increase in capture rate as a result of increased pressure in the absorber was recognized, as a cause of increased solubility of CO_2 at higher pressures. Increased pressure in the stripper column was identified as a parameter favorable for increased heat integration of the system.

Keywords: Aspen Plus, Carbon capture, Chemical absorption, MDEA, PZ.

Acknowledgements

This master thesis was carried out at RISE. We would especially like to thank our supervisors at RISE, Sima Ajdari and Maja-Stina Svanberg Frisinger, for their help, guidance, and encouragement throughout the thesis. We would also like to thank Phoenix BioPower for showing interest in our work and providing us with useful knowledge. Thanks to our examiner, Martin Seemann, for valuable inputs and insightful discussions during our work. We would also like to thank Wera Larsson for giving us helpful feedback on the report and the presentation. A special thanks to our family and friends, who have supported us greatly during our work.

A majority of the work was conducted at the Division of Energy Technology. We are very grateful for this opportunity, and would like to thank all people we have met there for fruitful and inspirational coffee talks.

Jesper Larsson, Tove Larsson, Gothenburg, June 2022

List of Abbreviations

Below is the list of abbreviations that have been used throughout this thesis listed in alphabetical order:

aMDEA	Activated N-Methyldiethanolamine
BTC	Biomass-fired Top Cycle
CHP	Combined Heat and Power
CSTRs	Continuous Stirred-Tank Reactors
elec-NRTL	Electrolyte Non Random Two Liquid property method
HSS	Heat Stable Salts
HT-WGS	High Temperature Water Gas Shift
LT-WGS	Low Temperature Water Gas Shift
MEA	Monoethanolamine
MDEA	N-Methyldiethanolamine
NOx	Nitrogen oxides
PSA	Pressure Swing Adsorption
PZ	Piperazine
SOx	Sulphur oxides
WGS	Water Gas Shift

Contents

List of Abbrevations **ix**

List of Figures **xiii**

List of Tables **xv**

1 Introduction **1**
1.1 Aim and scope . . . 2

2 Background **3**
2.1 Bio-FlexGen . . . 3

3 Theory **5**
3.1 Biomass gasification . . . 5
3.1.1 Environmental impact of bioenergy negative emission technologies . . . 5
3.2 Syngas cleaning . . . 6
3.2.1 Tar removal . . . 6
3.2.2 Water-gas shift . . . 7
3.3 Carbon capture . . . 7
3.3.1 Solvent based carbon capture . . . 8
3.3.1.1 Amine based solvents . . . 10
3.3.1.2 Amine degradation, emissions and environmental impact . . . 11
3.4 Pressure swing adsorption . . . 12
3.5 Applications for hydrogen . . . 12

4 Process modeling and methodology **15**
4.1 Process description . . . 15
4.2 Syngas treatment and WGS model . . . 16
4.3 Chemical absorption models . . . 18
4.3.1 Thermodynamics and kinetics . . . 18
4.3.2 Rate-based modelling . . . 21
4.3.3 Modelling procedure . . . 22
4.3.4 aMDEA model . . . 24
4.4 Parameter study . . . 26
4.5 Energy minimization . . . 26

5 Analysis and Discussion **29**
5.1 Parameter study 29
5.1.1 Solvent composition and flow 29
5.1.2 Pressure 30
5.1.2.1 Absorber pressure 30
5.1.2.2 Stripper pressure 31
5.1.3 Temperature 32
5.1.3.1 Absorber feed temperature 32
5.1.3.2 Stripper feed temperature 33
5.2 Optimization 34
5.2.1 Energy minimization 34
5.2.2 Model comparison 36

6 Conclusion **37**

7 Future work **39**
7.1 Model and methodology improvements 39
7.2 Research questions 39

Bibliography **41**

List of Figures

2.1 Schematic diagram of the operational mode including hydrogen production. The figure is adapted from fig. 6 Illustration of the hyflex btc mode of operation from the Bio-FlexGen grant agreement [1]. . . 3
2.2 Schematic diagram of the hydrogen production process. 4

3.1 General schematic of a chemical absorption based CO_2 capture process. 8

4.1 Schematic diagram of the hydrogen production process. 15
4.2 Aspen Plus flowsheet of the WGS model. 16
4.3 Aspen Plus flowsheet of the aMDEA open model. 24
4.4 Aspen Plus flowsheet of the aMDEA recirculated model. 25

5.1 The influence of varying solvent flow rate and composition on capture rate and absorption efficiency. 29
5.2 The influence of varying pressure in the absorber on capture rate and rich loading. 31
5.3 The influence of varying pressure in the stripper on capture rate and lean loading. 32
5.4 The influence of varying feed temperature into the absorber on capture rate and rich loading. 33
5.5 The influence of varying inlet temperature to the stripper column on capture rate and lean loading. 34
5.6 Heat demand in the carbon capture process for different liquid-to-gas ratios. Each line represents different pressure in the stripper column. 35

List of Tables

3.1 General reactions for amine based chemical absorption CO_2 capture [2]. 10

4.1 The syngas composition from the output stream of the gasification model. 16
4.2 Homogeneous gas phase reactions considered in the tar reforming unit [3]. 17
4.3 Syngas composition after WGS reactors. 17
4.4 Global reactions considered for the carbon capture model [4]. 18
4.5 Reactions condidered for the reactive absorption and desorption included for the absorber and stripper models [4]. 19
4.6 Pre-exponential factors, k, and activation energies, E, for rate-controlled reactions in the aMDEA process [4]. 20
4.7 Model parameters used in the aMDEA model. 22
4.8 Component groups used to calculate CO_2 loading. Where x represents the molar fraction of each respective component. 23
4.9 Fixed parameters in the aMDEA model. 24
4.10 Parameters varied in the parameter study including the intervals investigated. 26

5.1 The difference in process parameters and energy requirement for the base model and the final optimized model. 36

1
Introduction

The anthropogenic influence on the natural carbon cycle has been a growing issue since the beginning of the Industrial Revolution. Combustion of fossil fuels have contributed to a linear flow of carbon dioxide to the atmosphere causing climate change and projected negative consequences such as rising sea levels, agricultural drought and more intense storms [5]. In recent decades, population growth and industrial expansion have led to an increased energy demand, which has resulted in a continuous increase in annual global carbon dioxide emissions. Due to this, mitigation of CO_2 emissions is one of the most important and acute challenges that the world is facing today [6].

In order to achieve a sustainable energy sector and to mitigate climate change, fossil-based energy solutions need to be replaced. Possible replacements are renewable energy sources such as wind, solar and biobased energy . The transition however could result in a less flexible energy system due to the intermittency of some renewable energy sources [7]. Thus, decarbonization of the energy system also requires technical solutions that maintain grid stability and energy security. Biobased energy production combined with carbon capture technologies is a solutions that could support intermittent generation and retain flexibility in the energy system [7].

This master thesis project is a part of the Bio-FlexGen EU research project and was carried out with supervisors from the division Process- och systemanalys at RISE. The aim of the Bio-FlexGen EU project is to develop a flexible and efficient combined heat and power plant system using a Biomass-fired Top Cycle (BTC) and thereby combining gasification with gas turbine technology [7]. Some issues that the project want to address is security of supply, cost-effectiveness of combined heat and power (CHP) plants and flexibility and robustness towards energy fluctuations. This for example involves assuring that energy demands are met despite larger intermittency from increased variable renewable energy integration as well as developing CHP technology to achieve better electrical efficiencies and fast-start capability. The combination of gasification and gas turbine technology will allow the use of hydrogen and biomass as fuels. Hydrogen offers the possibility of fast dispatch of energy, and biomass contributes with lower operating costs. To examine the performance of the BTC plant, different operational modes are investigated in the project. One being the addition of a hydrogen production unit combined with carbon capture technology. In this master thesis project, the hydrogen production unit including carbon capture is modeled using the software Aspen Plus. The method used for carbon capture is chemical absorption using activated N-methyldiethanolamine (aMDEA)

as solvent.

1.1 Aim and scope

The aim of this master thesis is to develop a hydrogen production unit model for the BTC plant in the Bio-FlexGen project, which includes modelling of water-gas shift reactors and chemical absorption based carbon capture using the simulation software Aspen Plus. The purpose is to evaluate the absorption based aMDEA process through a conceptual modeling study.

The evaluation consist of a parameter study and an optimization. The parameter study is aimed to identify process parameters that ensure optimal absorption and desorption performance and thereby achieve a high carbon capture efficiency. Investigated process parameters are solvent flow rate and composition, pressure levels and feed temperatures. The goal with the optimization is minimizing energy consumption for solvent regeneration while obtaining a 90% carbon removal.

2
Background

2.1 Bio-FlexGen

The Bio-FlexGen project aims to develop a biomass fired top-cycle (BTC) plant, including a hybrid fluidized bed biomass gasification system and a top-cycle gas turbine. The BTC plant will be scalable and may include different configurations to ensure flexibility toward market fluctuations, such as electricity, peak electricity and CO_2 prices. The more advanced plant configuration includes a hydrogen production unit and a representation of that plant configuration is shown in figure 2.1. Hydrogen may be produced either in an electrolyser using renewable energy from wind or solar sources or in the hydrogen production unit. Syngas is produced through gasification of biomass, using oxygen provided by the electrolyser. The syngas can be used in the top cycle or be sent to the hydrogen production unit which in addition to hydrogen production include carbon capture. Hydrogen produced in the plant may be used in the top cycle gas turbine or in other industrial applications. The BTC plant will allow the top cycle turbine to have a fast start up time and will be able to quickly switch between fuels. The dynamic use of fuels will allow the system to have a flexible operation, which will optimize the economic performance of the system [1].

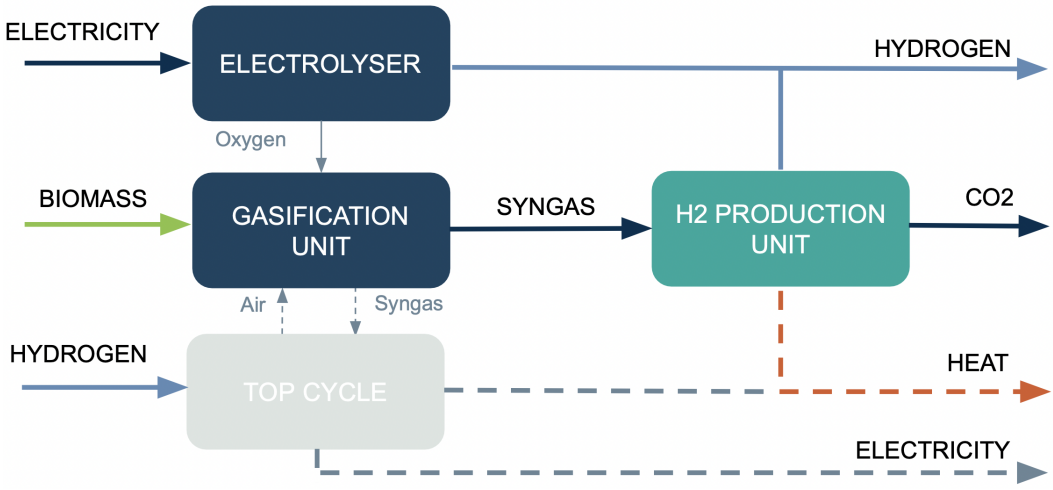

Figure 2.1: Schematic diagram of the operational mode including hydrogen production. The figure is adapted from fig. 6 Illustration of the hyflex btc mode of operation from the Bio-FlexGen grant agreement [1].

Included in this thesis is the BTC hydrogen production unit, visualized in figure 2.2.

The hydrogen production process involves syngas production through gasification of biomass, syngas treatment, water-gas shift (WGS) reactors, chemical absorption based carbon capture and pressure swing adsorption. The process is further described in section 4.1 and a theoretical background for the respective processes is included in chapter 3. The gasification unit is outside the system boundary of the thesis project and the models conducted include the subsequent process steps with the main focus on the carbon capture unit.

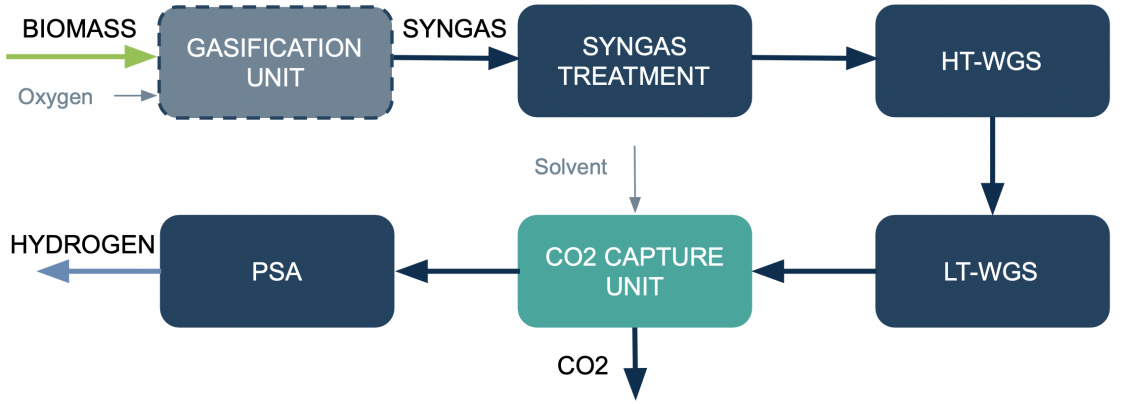

Figure 2.2: Schematic diagram of the hydrogen production process.

3
Theory

3.1 Biomass gasification

Gasification of biomass is a process which involves incomplete combustion of a solid bio-based fuel where combustible gases are produced. The gaseous mixture produced is commonly referred to as syngas. Gasification combined with subsequent syngas processing can generate biofuels such as methanol, Fischer-Tropsch fuels and hydrogen [8].

The thermochemical process of partial oxidation can utilize air, oxygen, steam or carbon dioxide as gasifying agents or a mixture of those components. Using oxygen instead of air as gasifying agent increases the heating value of the syngas produced, since the high nitrogen content of air lowers the heating value. The operational costs however increases due to production of oxygen being expensive. The benefit of using steam is increased heating value of the syngas and higher hydrogen content compared to air blown gasification. Using CO_2 helps conversion of char, tar and CH_4 into H_2 and CO with the downside that the process requires external heat supply [8].

Conversion of solid biomass fuel into syngas begin with a drying process, where water vapor is released from the surface and inner pore structure of the biomass. Subsequently, by an increase of temperature the structure of the solid fuel undergoes a transformation during devolatilization and pyrolysis. The prevalent products produced are light gases, tar and char with the main components being H_2, CO, CO_2, H_2O, CH_4 and other hydrocarbons. Afterwards, the gasification process starts, where the solid fuel (or the produced char) react with the externally added gasifying agent or the components of the gaseous mixture produced during drying and pyrolysis. These reactions generally occur at temperatures above 700 °C [8].

3.1.1 Environmental impact of bioenergy negative emission technologies

As a way of mitigating climate change, negative emission technologies using biomass could contribute to obtain a carbon neutral energy system. There are however uncertainties with regard to negative externalities that may arise from large scale expansion of bioenergy with carbon capture and storage [9, 10].

Historically, unsustainable biomass extraction has had negative impacts on natu-

ral ecosystems and social equity. Some negative impacts are loss of natural forests, degradation of productive land, decreasing carbon stocks, biodiversity losses, reduction of water resources and large greenhouse gas emissions due to land use change [9, 10].

There are however sustainable management strategies for bioenergy crop production which aim at minimizing the negative impacts. One example is conservation agriculture, where methods to avoid soil disturbance are used (i.e. no tillage practices). It also includes crop rotation and restoration of soil cover. Another strategy is introduction of smart technologies to use water and nutrients more efficiently. Additionally, using organic waste residues instead of bioenergy crops, such as by-products from food and fodder production and forest residues, could potentially lower the environmental impact [9]. The CHP plant developed in the Bio-FlexGen project will for example use residual non-food biomass, primarily forest residues and wood waste [11, 12].

3.2 Syngas cleaning

3.2.1 Tar removal

One main technical challenge with gasification of biomass is the formation of tars which can cause problems in the downstream equipment used for syngas processing. Tar formation could for example lead to clogging and blockages. Tars consist of heavy aromatic hydrocarbons, some examples being pyridine, toluene and naphthalene [13]. The general technical definition of tars is all organic compounds with higher molecular weight than benzene. However, benzene is normally accounted for as tar content in gasification systems due to the concentration of benzene usually being relatively high [14].

There are two main categories of tar removal technologies, thermal cracking and catalytic reforming, the latter being the most frequently used due to its lower operating temperature [15]. Thermal cracking involves a degradation process of tars, meaning that the heavy hydrocarbons transform into lighter hydrocarbons such as carbon monoxide and hydrogen. In order to degrade tars, high temperatures are required. For example, naphthalene degrades at 1300 °C and toluene at 950 °C. In this process however, tars are effectively removed [14].

Catalytic reforming means that the tars react with reforming agents (e.g., steam or CO_2) forming CO and H_2 as products. It can remove 95% of the tar from the process, with operating temperatures between 650-900 °C [13, 14]. A problem with catalytic reforming, using steam as reforming agent, is coke deposition that leads to deactivation of the catalysts. Hence, an important factor to abate this is to control the steam to carbon ratio [14].

3.2.2 Water-gas shift

For various industrial applications where the produced syngas or pure hydrogen is used, the H_2/CO ratio in the syngas is a crucial factor [15]. To shift this ratio it is possible to use water-gas shift (WGS) reactors to convert parts of the carbon monoxide with steam, into carbon dioxide and hydrogen via reaction 3.1. This reaction also makes it possible to capture more CO_2, as CO_2 yields increase when CO is converted. WGS-reactors usually utilizes two types of catalysts, high temperature WGS catalysts with operating temperatures between 310-450 °C and low temperature WGS catalysts that operate between 150-250 °C [15].

$$CO + H_2O \leftrightarrow H_2 + CO_2 \tag{3.1}$$

The water-gas shift reaction is a reversible and moderately exothermic reaction with a heating value of $\Delta H = -41.1\,kJ/mol$ at $298\,K$. Thermodynamically, this means that low temperatures are beneficial for the conversion of CO. However, the reaction rate at low temperatures is slow. In order to optimize hydrogen yields it is therefore common to use two water-gas shift reactors, one high-temperature reactor (HT-WGS) and one low-temperature reactor (LT-WGS). The syngas first enter the HT-WGS, and when the CO conversion has reached a point where the backwards reaction is starting to take over, the gas leaves the high-temperature reactor in order to be cooled and then enter the reactor that operates at a lower temperature. This procedure allows the hydrogen yield to increase, compared to only using one reactor [15].

3.3 Carbon capture

Carbon capture and storage technologies are methods developed with the goal of mitigating emissions from processes where carbon dioxide is a by-product. The three main categories of carbon capture are pre-combustion, post-combustion, and oxyfuel carbon capture. Other methods are investigated globally, but most of them have not reached a point where they are ready to be applied to industrial applications [16].

Post-combustion carbon capture is a process where CO_2 is captured from the flue gases after the combustion of a fuel. Pre-combustion carbon capture are technologies where CO_2 is captured before the combustion of a fuel is complete. It may for example be carbon capture technologies applied in gasification processes. The gasification yields a syngas stream from which CO_2 is removed and hydrogen or a hydrogen rich gas is produced. Oxy-fuel combustion is a process where fuel is combusted in an environment of pure oxygen instead of air. This creates a flue gas mainly consisting of CO_2 and water vapor. The water in the gas can be separated from the CO_2 by condensation, which yields a pure CO_2 stream [16].

Carbon that is captured in carbon capture processes can either be stored or utilized. The CO_2 can be used in various industrial applications, such as hydrogenation of CO_2 in order to produce methanol, methane and other hydrocarbons. CO_2 is also

commonly used as a refrigeration agent and enhancer of oil recovery, among other utilizations [17].

3.3.1 Solvent based carbon capture

A method that may be used for post-combustion as well as pre-combustion capture is solvent based capture where several different solvents may be used as capture media for the CO_2. A common absorption technology is wet scrubbing using amine based solvents. It is a technology that mainly has been applied for gas sweetening of flue gases from coal fired power plants but it has also been used in natural gas fired processes. For bioenergy applications it is however fairly new [9]. Another option besides amine based wet scrubbing, is physical absorption where physical solvents absorb CO_2 under high pressure conditions ($>$ 20 bar) [18].

Carbon capture using amine-based solvents is a cyclic process where CO_2 is absorbed into a relatively cold amine solution in an absorption column and after which the solution is heated and the CO_2 is released from the solution in a desorption column. The solvent is thereby regenerated [2]. In Figure 3.1 a general schematic of a solvent-based chemical absorption process is shown. The gas mixture and the lean solvent enters a packed column, an absorber. The gas enters at the bottom of the column and the amine solution at the top. The packing material creates a large surface area where the counterflowing liquid and gas reacts. The remaining gas with low CO_2-content exits at the top of the column. The solvent loaded with CO_2 exits at the bottom of the absorber and is called the rich solvent stream. It is pumped to a desorption column, a stripper, before which it is heated in a cross heat exchanger. During the desorption in the stripper, the rich solvent is heated by the reboiler, generating a stream of CO_2 with high purity which is cooled in a condenser to remove water and solvent that may be present. The lean solvent exiting the stripper is recirculated. Before entering the absorber, heat is recovered from the stream via a cross-exchanger and the lean solvent is also further cooled before being returned to the absorber [9]. During the cycles where the solvent is heated and cooled multiple times, it starts to degrade and must therefore be replaced regularly to achieve sufficient absorption performance. Solvent make up is also required to compensate for the losses in the output streams of the respective columns. The process is energy intensive, mainly due to the heat duty of the reboiler in the stripper [9].

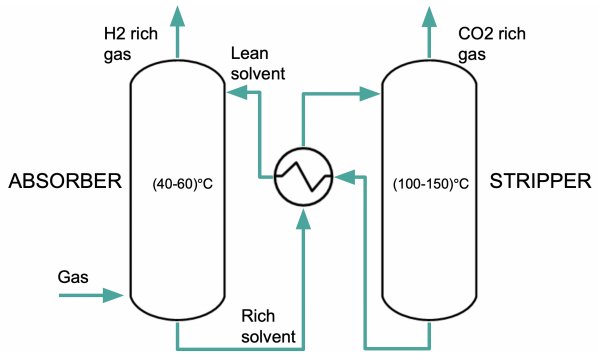

Figure 3.1: General schematic of a chemical absorption based CO_2 capture process.

The absorption process involves mass transfer of CO_2 from the gas phase to the liquid phase which is controlled by dissolution and diffusion. When $CO_{2(g)}$ and the aqueous amine solution are contacted, there is a concentration gradient providing a driving force, making the CO_2 diffuse into the solvent. This driving force is represented by the mathematical expression in equation 3.2 and exist until equilibrium is reached. When CO_2 in gas-phase has dissolved, the low concentration of CO_2 near the interface results further increase the driving force that transfers CO_2 from the gas bulk to the gas-liquid interface [2].

$$\text{Driving force} = P_{CO_2} - P^*_{CO_2} \tag{3.2}$$

P_{CO_2} is the concentration of CO_2 in gaseous form and $P^*_{CO_2}$ is the concentration of dissolved CO_2, both represented by partial pressure where $P^*_{CO_2}$ is referred to as the equilibrium partial pressure. or each temperature, the relationship between the equilibrium partial pressure and the so called equilibrium concentration $[CO_2]^*$ descibed by equation 3.3 remain constant[2].

$$h_{CO_{2,L}} = \frac{P^*_{CO_2}}{[CO_2]^*} \tag{3.3}$$

The constant $h_{CO_{2,L}}$ is referred to as the Henry constant and describes the solubility of carbon dioxide in a liquid L. With solubility being the amount of CO_2 that may be dissolved into the aqueous solution until it is saturated [2].

The rate of diffusion, i.e. the rate which CO_2 molecules diffuse through the gas and liquid phases, is what controls the time needed to reach equilibrium. In the gas phase, the rate of diffusion is high due to molecules moving around more freely and having higher kinetic energy. Hence, the diffusion rate in the liquid phase is what limits the time to reach equilibrium. The diffusion in the liquid phase is limited by the liquid viscosity and the volume of the diffusing gas molecule.

Apart from diffusion and solubility, the chemical reactions occuring in the aqueous amine solution also have an impact of the mass transfer of CO_2. Once dissolved, the CO_2 reacts with the amine solution. As long as the reactions occur, this entails a lower concentration of CO_2 in the gas-liquid interface, thereby further ensuring a driving force for CO_2 transport to the liquid phase.

When the CO_2 from the flue gas or syngas is absorbed into the aqueous solution it reacts with the amine, water and hydroxide. The general reactions for chemical absorption are presented in Table 3.1. The amine reaction is selective towards acid gases, such as CO_2 and H_2S, and the amines do not react with the other compounds in the gas. The relatively low temperature in the absorber ensures a high affinity for CO_2 absorption instead of H_2S absorption. Reactions 3, 4, 5, 6, and 8 are instantaneous protonation equilibria reactions, whereas reaction 1, 2 and 7 are relatively slow in comparison [2].

Table 3.1: General reactions for amine based chemical absorption CO_2 capture [2].

No.	Reaction
1	$CO_2 + H_2O \longleftrightarrow H_2CO_3$
2	$CO_2 + OH^- \longleftrightarrow HCO_3^-$
3	$CO_3^{2-} + H^+ \longleftrightarrow HCO_3$
4	$HCO_3^- + H^+ \longleftrightarrow H_2CO_3$
5	$RNH_2 + H^+ \longleftrightarrow RNH_3^+$
6	$OH^- + H^+ \longleftrightarrow H_2O$
7	$CO_2 + RNH_2 \longleftrightarrow RNHCO_2H$
8	$RNH_2CO_2^- + H^+ \longleftrightarrow RNH_2CO_2H$

The efficiency of chemical absorption to separate CO_2 from a gaseous mixture depends on for example chemical reaction rates, diffusion rates, chemical equilibria, heat capacity, viscosity and solubility. It also depends on the temperature dependency of said properties [2].

In the desorption column, the higher temperature entails lower solubility for CO_2, resulting in the release of CO_2 from the solution. Diffusion is the limiting factor for desorption and the reverse reactions are fast. However, a large amount of heat is required due to desorption being endothermic [2].

3.3.1.1 Amine based solvents

Several alkanolamine-solvents can be used in chemical absorption processes, the most commonly used is an aqueous solution of monoethanolamine (MEA) [2]. Some main solvent properties beneficial for chemical absorption are high loading capacities, low energy requirement for regeneration, reactivity with CO_2 and high stability [19].

Alkanolamines can be divided into primary, secondary, tertiary, cyclic and sterically hindered amines. Primary and secondary amines, such as MEA and diethanolamine, have higher reaction rates and hence faster absorption. Tertiary and sterically hindered amines require less energy for regeneretaion and thereby have lower stripping cost [19, 20]. MEA and the tertiary amine N-Methyldiethanolamine (MDEA) are two commercially available amines frequently used in industry [19]. MEA is cheap and easy to produce and has a a high reaction rate with CO_2. It is however not suitable for high pressure applications and cause problems with corrosion [20]. MDEA is favorable due to its higher CO_2 loading capacity, low corrosivity and that it is

less vulnerable to degradation and hence have lower solvent loss. It does however have lower reactivity with CO_2 [20, 21]. Piperazine (PZ) is a commonly used cyclic secondary amine with a very high reaction rate (more than double compared to MEA) and strong resistance towards thermal degradation. PZ can be used with temperatures up to 150 °C, compared to for example MEA that degrades at 120 °C. PZ however has the main disadvantage that it can cause solids to form at low temperatures (below 0 °C) combined with either low or high CO_2 loading [19, 20].

Blending different amines could decrease energy requirements and reduce negative impacts such as corrosion and emissions to atmosphere due to degradation [21]. PZ can for example be used to increase the absorption rate of other solvents, such as MDEA. The mixed aqueous solution of MDEA and PZ is commonly referred to as activated MDEA or aMDEA [22, 23]. Furthermore, it can minimize the thermal degradation of MDEA. Optimization of MDEA and PZ concentrations in the solution could also help reduce reboiler heat duty [23].

3.3.1.2 Amine degradation, emissions and environmental impact

Degradation products from amine-based solvents can cause corrosion and reduce the energy efficiency of the chemical absorption process. Additionally, environmental problems can rise as a result of emissions to the environment. Two main degradation mechanisms are oxidative degradation and thermal degradation [24].

Oxidative degradation mainly occur during absorption, due to presence of oxygen in the gas stream. During oxidative degradation, volatile amines and aldehydes are formed. The aldehydes can subsequently oxidize rapidly and form acids that can cause corrosion and fouling [25]. Furthermore, heat stable salts (HSS) can form during absorption and accumulate in the process equipment and result in a solvent loss [24]. Thermal degradation, also referred to as carbamate polymerization, mainly occur during desorption, due to higher temperatures (120-150 °C) in the stripper [25, 26]. It may also occur in the cross heat exchanger. The degradation products from thermal degradation lowers the capacity of CO_2 capture which is why it is necessary to include a purge stream discarding some used solvent and also to add new solvent via a make up stream [26].

A main concern related to CO_2 capture technology is some degradation products being volatile, causing significant solvent loss. Additionally, toxic heavy metals from flue gas or syngas and corrosion inhibitors used can be emitted to the environment [26]. The degradation products nitrosamines and nitramines can potentially pollute air and drinking water supplies. Nitrosamines can be carcinogenic, toxic and mutagenic, hence can pose a potential threat to human health and ecosystems [26].

Examples of strategies for managing and minimizing amine degradation are selection of amines that are resistant to degradation, use of additives that prevent corrosion and oxidation and pretreatment of the gas stream [24]. The selection of amines with the objective of minimizing degradation is not only an important strategy for reducing the environmental impact, the need for solvent make up can also be an

economical concern. Studies have shown that as much as 10% of the total operating cost of chemical absorption units using MEA can be related to solvent make up [26]. Solvents that are more susceptible to oxidative degradation are primary and secondary amines, making sterically hindered and tertiary amines better choices when minimizing degradation [24]. Blending a thermally stable solvent such as PZ to other amines, such as MEA and MDEA, can reduce thermal degradation [26]. Sulphur oxides (SOx) and Nitrogen oxides (NOx) that may be present in the gas stream can have a negative impact on the CO_2 absorption capacity and the environment. SO_2 can for example cause formation of HSS and increase degradation rates and NOx can react with amines and form nitrosamines and nitramines. It is therefore important to have proper pretreatment of the gas stream to decrease the amount of SOx and NOx present in the chemical absorption process [26].

3.4 Pressure swing adsorption

Pressure swing adsorption (PSA) is a widely implemented technology for gas separation, with fairly low operating and maintenance costs. It can be used to separate H_2 from various gas mixtures. PSA units contain solid packed beds and can produce a very pure hydrogen stream (99-99.999+%) with hydrogen recovery of 60-90% [27, 28]. Different adsorbents can be used in the process, and the choice of adsorbents has a great impact on the separation efficiency. Some common adsorbents are silica gel, activated carbon and zeolites and they all have strong adsorption affinity for the impurities in the gas stream. The different adsorbents however are more or less suitable to handle different types of impurities, making multi-layered beds including different adsorbents more efficient and more widely used. Operating temperatures for adsorption are often around ambient temperature (290-310 K) and operating pressures are normally around 10-40 bar, but may also be as low as 5 bar and as high as 65 bar [27].

3.5 Applications for hydrogen

To mitigate climate change, hydrogen has been recognized as a fuel that may become a substitute for fossil based ones. It has been projected that H_2 can become commercially mature in the energy sector by 2030 [27]. An issue is however that the majority of hydrogen produced today is produced from fossil fuels. Only 2% are produced using electrolysis and 0.7% is produced from renewables or fossil fuel plants using carbon capture utilization and storage technologies [29].

Today, the main applications for hydrogen are in the industry, for example oil refining, ammonia production, methanol production and steel production. Hydrogen is an element with high specific energy, making it attractive for applications in the transport industry. It does however have a low energy density, meaning that large volumes are required compared to other fuels when supplying a certain energy demand, making it more suitable for large vehicles. Hydrogen may also become an important fuel for heat and power generation. Different applications require more

or less pure hydrogen. Methanol synthesis and energy production do not require pure hydrogen, whereas hydrogen need to be ultra-pure (99.99+%) when used in refineries, ammonia synthesis and fuel cells [27, 29].

4

Process modeling and methodology

4.1 Process description

In this thesis, models for a hydrogen production process are constructed using the simulation software Aspen Plus. Figure 4.1 visualizes the process considered as a schematic diagram. The gasification unit is not included in the system boundary for this thesis, and the input syngas stream used is given from an existing gasification model. Syngas produced in the gasification unit is treated in order to remove tars after which the composition of the gas is changed using two water-gas shift reactors, one high temperature reactor and one low temperature reactor. The gas exiting the second WGS is used as input for a chemical absorption based carbon capture model, which uses the ammonium based solvent aMDEA. The carbon capture unit includes two product gas streams, one mainly consisting of CO_2 and the other being a hydrogen rich syngas stream. After CO_2 removal, the hydrogen rich gas is fed to a pressure swing adsorption unit, where a pure hydrogen stream is produced. In section 4.2 and section 4.3.4, the respective models are further described. The primary focus for this thesis has been the construction and evaluation of the carbon capture model.

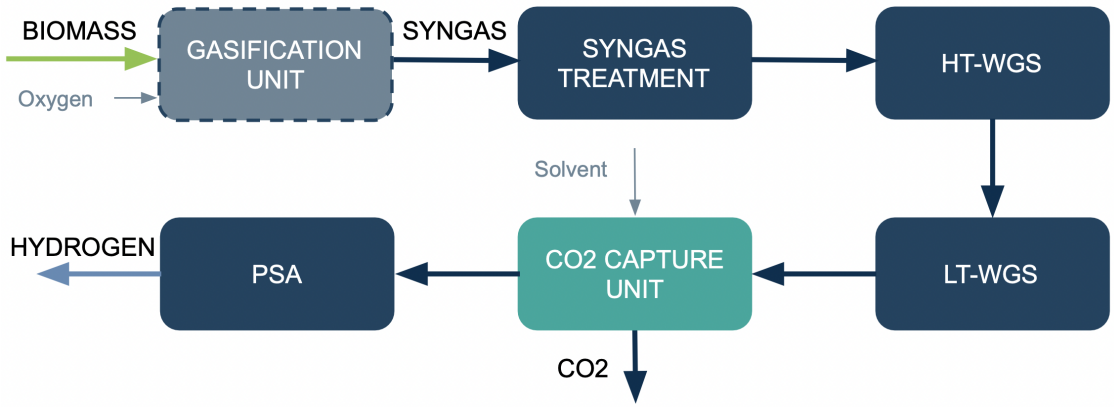

Figure 4.1: Schematic diagram of the hydrogen production process.

The gas composition from the gasification system is presented in Table 4.1. A gas cleaning unit removing hydrogen sulfide is included in the gasification system and the resulting H_2S concentration is assumed to be negligible. The tar was assumed to consist of only benzene. It is a common approximation to combat the difficulty of modeling accurate tar compositions and significantly decrease computational time [3]. In reality, tar is a complex mixture of different multi-ring aromatic hydrocarbons [3].

Table 4.1: The syngas composition from the output stream of the gasification model.

Component	Mole fraction
H_2	0.2813
CO_2	0.1973
H_2O	0.0976
O_2	0.0082
CO	0.3473
N_2	0.0005
CH_4	0.0543
C_2H_4	0.0119
C_6H_6	0.0016

4.2 Syngas treatment and WGS model

An equilibrium based WGS model including a tar reforming unit was conducted in Aspen Plus. It was modeled using the built in Aspen Plus property method PENG-ROB which uses the Peng-Robinson equation of state [30]. The process flowsheet of the WGS model is shown in Figure 4.4.

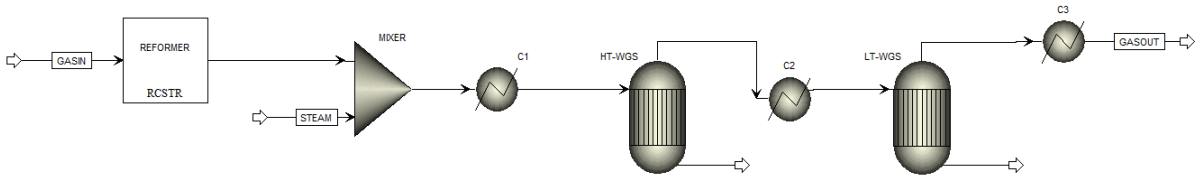

Figure 4.2: Aspen Plus flowsheet of the WGS model.

The gasification product stream is fed to a tar reforming unit, represented by an RCSTR block. The Aspen Plus RCSTR block rigorously models a continuous stirred tank reactor. Operating temperature and pressure of the tar reformer is set to 600 °C and 9 bar with reforming equations according to Table 4.2.

Table 4.2: Homogeneous gas phase reactions considered in the tar reforming unit [3].

No.	Reaction	Arrhenius expression ($\mathrm{mol\,m^{-3}\,s^{-1}}$)
1	$CH_4 + 1.5\,O_2 \longrightarrow CO + 2\,H_2O$	$3.0 \times 10^5 \cdot e^{-(\frac{15098}{T})} \cdot [CH_4] \cdot [H_2O]$
2	$C_2H_4 + 2\,O_2 \longrightarrow 2\,CO + 2\,H_2O$	$1.0 \times 10^{12} \cdot e^{-(\frac{20844}{T})} \cdot [C_2H_4] \cdot [O_2]$
3	$C_6H_6 + 4.5\,O_2 \longrightarrow 6\,CO + 3\,H_2O$	$7.59 \times 10^6 \cdot e^{-(\frac{24200}{T})} \cdot [C_6H_6]^{-0.1} \cdot [O_2]^{1.85}$
4	$C_6H_6 + 6\,H_2O \longrightarrow 6\,CO + 9\,H_2$	$3.0 \times 10^5 \cdot e^{-(\frac{15098}{T})} \cdot [C_6H_6] \cdot [H_2O]$

To achieve higher CO conversion, 2 kg/s steam with temperature 200 °C, is mixed with the syngas stream. The resulting gas stream is then cooled down to the operating temperature of the HT-WGS. To enhance the H_2/CO ratio further, two WGS reactors are used, one HT-WGS and one LT-WGS. REquil blocks are used to model the reactors. The REquil model in Aspen Plus calculates flow rates for the streams using equilibrium constants derived from Gibbs free energy. Included in the blocks is the water-gas shift reaction 4.1

$$CO + H_2O \leftrightarrow H_2 + CO_2 \tag{4.1}$$

The operating temperatures are 400 °C and 150 °C for the HT-WGS and the LT-WGS respectively. A CO conversion of 98% is achieved and the outlet composition of the syngas is presented in Table 4.3. Lastly, the resulting syngas stream is cooled down to the inlet temperature of the carbon capture unit, i.e. 40 °C.

Table 4.3: Syngas composition after WGS reactors.

Component	Mole fraction
H_2	0.47514
CO_2	0.41102
H_2O	0.05095
O_2	0.00600
CO	0.00489
N_2	0.00038
CH_4	0.04144
C_2H_4	0.00895
C_6H_6	0.00122

4.3 Chemical absorption models

The reaction kinetics models and the thermophysical property models used in this thesis are based on the works of Austgen [31], Bishnoi and Rochelle [32] and Hilliard [33].

4.3.1 Thermodynamics and kinetics

The electrolyte NRTL property method (elec-NRTL) was used in order to calculate liquid properties. It was coupled with the Redlich-Kwong equation of state [34] that allows computation of non-idealities in the vapor phase [4, 35]. In order to describe the solutes, Henry's law is applied. Henry constants are specified for the solutes with water, MDEA and PZ respectively according to the existing property model available in Aspen Plus [4].

The reaction chemistry was modeled using the global electrolyte calculation option as well as using a reaction model for the absorption and stripper column. The global reactions considered for the process are equilibrium reactions which are presented in Table 4.4. The reaction model for the absorber and stripper include equilibrium reactions as well as kinetic reactions and is presented in Table 4.5.

Table 4.4: Global reactions considered for the carbon capture model [4].

No.	Reaction	Stoichiometry
1	Equilibrium	$2\,H_2O \longleftrightarrow H_3O^+ + OH^-$
2	Equilibrium	$CO_2 + 2\,H_2O \longleftrightarrow HCO_3^- + H_3O^+$
3	Equilibrium	$HCO_3^- + H_2O \longleftrightarrow CO_3^{2-} + H_3O^+$
4	Equilibrium	$PZH^+ + H_2O \longleftrightarrow PZ + H_3O^+$
5	Equilibrium	$PZ + HCO_3^- \longleftrightarrow PZCOO^- + H_2O$
6	Equilibrium	$HPZCOO + H_2O \longleftrightarrow PZCOO^- + H_3O^+$
7	Equilibrium	$PZCOO^- + HCO_3^- \longleftrightarrow PZ(COO-)_2 + H_2O$
8	Equilibrium	$MDEAH^+ + H_2O \longleftrightarrow MDEA + H_3O^+$

Table 4.5: Reactions condidered for the reactive absorption and desorption included for the absorber and stripper models [4].

No.	Reaction	Stoichiometry
1	Equilibrium	$2\,H_2O \longleftrightarrow H_3O^+ + OH^-$
2	Equilibrium	$HCO_3{}^- + H_2O \longleftrightarrow CO_3{}^{2-} + H_3O^+$
3	Equilibrium	$PZH^+ + H_2O \longleftrightarrow PZ + H_3O^+$
4	Equilibrium	$HPZCOO + H_2O \longleftrightarrow PZCOO^- + H_3O^+$
5	Equilibrium	$MDEAH^+ + H_2O \longleftrightarrow MDEA + H_3O^+$
6	Kinetic	$CO_2 + OH^- \longrightarrow HCO_3{}^-$
7	Kinetic	$HCO_3{}^- \longrightarrow CO_2 + OH^-$
8	Kinetic	$PZ + CO_2 + H_2O \longrightarrow PZCOO^- + H_3O^+$
9	Kinetic	$PZCOO^- + H_3O^+ \longrightarrow PZ + CO_2 + H_2O$
10	Kinetic	$PZCOO^- + CO_2 + H_2O \longrightarrow PZ(COO-)_2 + H_3O^+$
11	Kinetic	$PZ(COO-)_2 + H_3O^+ \longrightarrow PZCOO^- + CO_2 + H_2O$
12	Kinetic	$MDEA + CO_2 + H_2O \longrightarrow MDEAH^+ + HCO_3{}^-$
13	Kinetic	$MDEAH^+ + HCO_3{}^- \longrightarrow MDEA + CO_2 + H_2O$

The method chosen for calculating the equilibrium constants was the standard Gibbs free energy change [4]. The expression for calculating the equilibrium constants is shown in equation 4.2:

$$K_{eq} = exp\left(\frac{\Delta G^0}{RT^L}\right) \tag{4.2}$$

where the values for the standard Gibbs free energy change, ΔG^0, are obtained from the Aspen Plus database [35]. R is the gas constant and T^L is the liquid temperature.

The rate of reaction for the kinetic reactions were calculated using power law expressions with the general equation being [4]:

$$r = k(T/T_0)^n exp\left[\left(\frac{-E}{R}\right)\left(\frac{1}{T} - \frac{1}{T_0}\right)\right]\prod_{i=1}^{N} C_i^{a_i}$$

Where:
r = Rate of reaction;
k = Pre-exponential factor;
T = Absolute temperature;
T_0 = Reference temperature;
n = Temperature exponent;
E = Activation energy;
R = Universal gas constant;
N = Number of components in the reaction;
C_i = Concentration of the component i;
a_i = The stoichiometric coefficient of component i in the reaction equation;

In this case, T_0 was unspecified, resulting in the use of the reduced power law expression shown in equation 4.4.

$$r = kT^n exp\left(\frac{-E}{RT}\right)\prod_{i=1}^{N} C_i^{a_i}$$

The concentration basis assumed is molarity and n is assumed to be 0. Table 4.6 shows the values used for pre-exponential factors and activation energy for the aMDEA process.

Table 4.6: Pre-exponential factors, k, and activation energies, E, for rate-controlled reactions in the aMDEA process [4].

No.	k	E [J/kmol]
6	4.23e+13	5.54709e+07
7	2.38e+17	1.23305e+08
8	4.14e+10	3.36548e+07
9	7.94e+21	6.59756e+07
10	3.62e+10	3.36548e+07
11	5.56e+25	7.69199e+07
12	2.22e+7	3.78026e+07
13	1.06e+16	1.06445e+08

4.3.2 Rate-based modelling

The absorption and stripper columns were simulated using the Aspen Plus RadFrac™ model. In order to give a better description of the non-idealities of reactive absorption and desorption, the rate-based approach was chosen instead of the equilibrium stages approach, which is also the method most commonly used for chemical absorption modelling in Aspen Plus today [35]. Historically, equilibrium-based models have been used as well, assuming thermodynamic equilibrium. This approach however, cause large discrepancies when describing reactive systems since limitations to mass transfer, such as reaction kinetics and film diffusion are not considered. Additionally, it has low accuracy when predicting reboiler duties, equipment sizes and temperature profiles in the absorption and desorption columns. It is therefore not suitable for simulating CO_2 absorption and desorption [36].

The rate-based approach is based on the two-film theory suggested by Lewis and Whitman [37]. The theory describes the mass transfer between two contacting phases, gas and liquid. At the gas-liquid interface, equilibrium is assumed, with concentration and temperature gradients assumed to be confined within the liquid and vapor films next to the interface [35, 38, 39]. The RadFrac™ columns, approximates a plug-flow reactor by adding a series of continuous stirred-tank reactors (CSTRs). The number of stages in the columns represent the number of CSTRs in series, thereby describing the discretization of the axial domain [35]. The model also considers electrolyte chemistry and hydrodynamics [40].

The model parameters used for the RadFrac™ columns are summarized in Table 4.7. The Bravo et. al correlation (1985) [41], the Chilton Colburn method [42] and the Billet and Schults (1999) Holdup correlation [43] were chosen to calculate the packing performance in the columns. The Bravo et. al correlation predicts mass transfer coefficients and interfacial area and is preferred for structured packing and the Chilton colburn method uses the binary mass transfer coefficients from the Aspen Plus databank to calculate heat transfer coefficients. The Billet and Schults correlation predicts liquid holdup in packed columns. The flow-model describes the bulk conditions for each stage. In this case the mixed flow model was used, which assumes equal inlet and outlet conditions for each stage.

Table 4.7: Model parameters used in the aMDEA model.

Model parameters	
Model approach	Rate-based calculation
Electrolyte simulation approach	True components
Flow-model	Mixed flow model
Film resistance liquid phase	Discretized film with 5 discretization points
Film resistance vapor phase	Film reactions
Mass transfer coefficient method	Bravo et al. correlation (1985) [41]
Heat transfer coefficient method	Chilton and Colburn Method [42]
Interfacial area method	Bravo et al. correlation (1985) [41]
Liquid holdup correlation method	Billet and Schultes (1999) Holdup Correlation [43]

4.3.3 Modelling procedure

Solvent flow rate, stripper reboiler duty and the condenser duty of the absorber were altered to achieve a CO_2 capture efficiency of 90%. The set value of 90% was chosen since studies have shown that the reboiler duty has an almost linear increase until it reaches 90% capture, after which the reboiler duty increases exponentially [9]. The capture efficiency was calculated using equation 4.5.

$$\text{Capture rate} = \frac{G_{out} x_{\text{CO}_2 out}}{G_{in} x_{\text{CO}_2 in}} \cdot 100\% \tag{4.5}$$

where G_{in} is the mass flow of of the inlet syngas stream to the process and G_{out} is the mass flow of outlet stripper gas stream. x_{CO_2} is the mole fraction of CO_2 in the separate gas streams.

When the solvent flow-rate was altered, the dimensions, height and diameter, of the absortion and stripper columns were also changed to achieve adequate hydraulic plots.

The CO_2 loading was calculated using equation 4.6 for the aMDEA process. It is defined as the ratio between the apparent molar fractions of CO_2 and amines. In Aspen a property set, ML-LOAD, was created to obtain the results of CO_2 lean loading and CO_2 rich loading for every simulation. Two component groups were

constructed for the property set, $x^{app}_{CO_2}$ and x^{app}_{aMDEA}, which are given in Table 4.8. The property set was then added to the report page for each column. The value for lean loading, is the reported value from ML-LOAD at stage 20 in the stripper and rich loading is the reported value at stage 20 in the absorber. Rich and lean loading are used to describe the performance of each of the columns.

$$Loading = \frac{x^{app}_{CO_2}}{x^{app}_{aMDEA}} \tag{4.6}$$

Table 4.8: Component groups used to calculate CO_2 loading. Where x represents the molar fraction of each respective component.

$x^{app}_{CO_2}$	x^{app}_{aMDEA}
x_{CO_2}	x_{MDEA}
$x_{HCO_3^{2-}}$	x_{MDEAH+}
$x_{CO_3^{2-}}$	x_{PZ}
x_{HPZCOO}	x_{PZH^+}
x_{PZCOO^-}	x_{HPZCOO}
$x_{HPZCOO^{2-}}$	x_{PZCOO^-}
	$x_{HPZCOO^{2-}}$

Another way to quantify the absorption performance, apart from the rich loading factor, is through the absorption efficiency, which is calculated using equation 4.7

$$\text{Absorption Efficiency} = \frac{G_{in}x_{\mathrm{CO_2}in} - G_{abs}x_{\mathrm{CO_2}abs}}{G_{in}x_{\mathrm{CO_2}in}} \cdot 100\% \tag{4.7}$$

where G_{in} is the mass flow of the syngas entering the absorber and G_{abs} is the mass flow of the hydrogen rich syngas leaving the absorber. $x_{\mathrm{CO_2}}$ is the mole fraction of CO_2 in the different gas streams.

In order to get the recirculated systems to converge, models without recirculation were created first. The aMDEA model without recirculation, referred to as the aMDEA open model, is shown in Figure 4.3. These models included calculators for the make up streams, in order to compensate for solvent and water losses. The calculated stream properties for open model lean solvent stream (LEANIN-R), were used as input for lean solvent stream (LEANIN) in the recirculated model. The results from the make up stream calculators were also used as input for the closed loop model since the calculators created difficulties with convergence and significantly increased the computational time in a recirculated model.

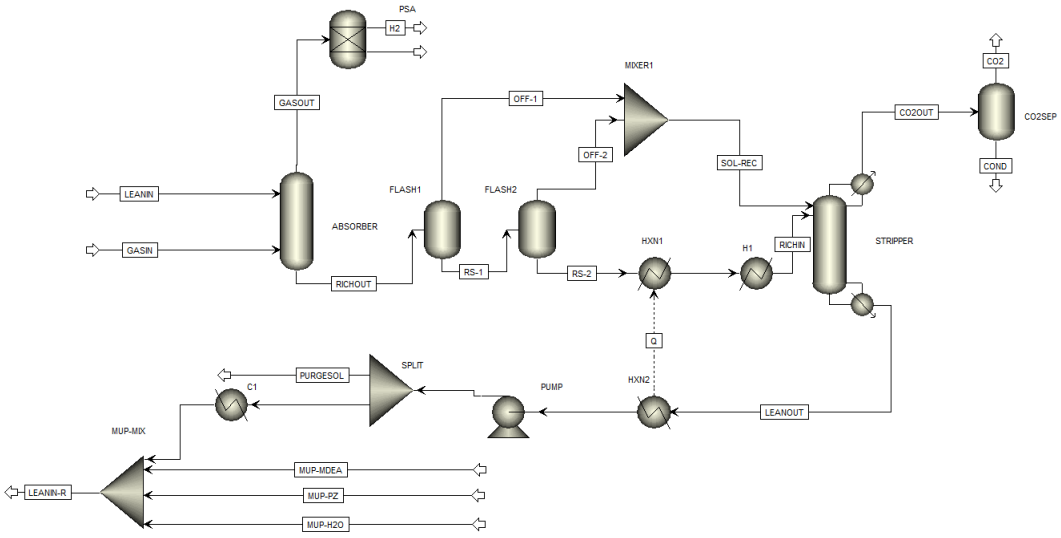

Figure 4.3: Aspen Plus flowsheet of the aMDEA open model.

4.3.4 aMDEA model

The absorber and stripper columns were simulated using 20 theoretical stages with dimensions and design parameters according to Table 4.9. The packing material used for the respective columns was Sulzer MELLAPAK with dimensions 250Y.

Table 4.9: Fixed parameters in the aMDEA model.

Simulation conditions	
Solvent flow rate [kg/s]	80.19
Syngas flow rate [kg/s]	10
L/G ratio [mass]	8.02
Absorber height [m]	12
Absorber diameter [m]	2.1
Stripper height [m]	11
Stripper diameter [m]	2.4
Reboiler duty [MW]	13
Condenser duty [MW]	0.3

In Figure 4.4 the aMDEA model is presented. The lean solvent stream (LEANIN) enters the absorber at stage 1 and the syngas stream (GASIN) enters the column at stage 20 both with inlet temperatures of 40 °C. In Table 4.3, the syngas composition can be found. The aMDEA solvent composition is 45 wt% MDEA and 5 wt% PZ. Pressure for the absorber and the inlet streams is set to 9 bar in order to simulate a high pressure system while staying within the limit where the binary coefficients from the Aspen Plus database are valid. The absorption column has a total cooling duty of 1.5 MW, equally distributed on stage 5, 10 and 15 to achieve lower temperatures and thereby more efficient absorption.

At the top of the absorber, a H_2 rich stream (GASOUT) exits which is fed to a PSA unit with inlet conditions of 45.33 °C and 9 bar. The PSA unit is simulated using a component separator block with an efficiency of 85%, creating a pure H_2 stream. After exiting the absorption column at the bottom, the rich solvent stream (RICHOUT) enters a flash tank (FLASH1) which decreases the pressure to 4 bar and subsequently an additional flash tank (FLASH2) further decrease the pressure to 1.6 bar. Thereafter, the off-gas from the flash tanks are mixed and fed to stage 1 in the stripper column and the rich solvent (RS-2) is heated via a cross heat exchanger.

An additional heat exchanger is used which increases the temperature to 100 °C before entering the stripper at stage 1. A minimum temperature difference in the cross heat exchanger of 10 °C is assumed. From the top of the stripper, a CO_2 rich gas stream (CO2OUT) exits which later enters a flash tank to condensate water and achieve a CO_2 stream with 90% purity. The lean solvent exiting at the bottom of the stripper (LEANOUT) is cooled in the cross heat exchanger before entering a pump, raising the pressure back to 9 bar.

A splitter is used to separate 1% of the spent solvent in a purge stream. The remaining 99% is further cooled to 40 °C, after which a mixer is used to add make up streams for MDEA, PZ and water. The make up streams are required to fulfil the mass balance in the recirculated system and make up for solvent losses in the absorber, stripper and the purge stream. The solvent stream leaving the mixer is then recirculated into the absorber.

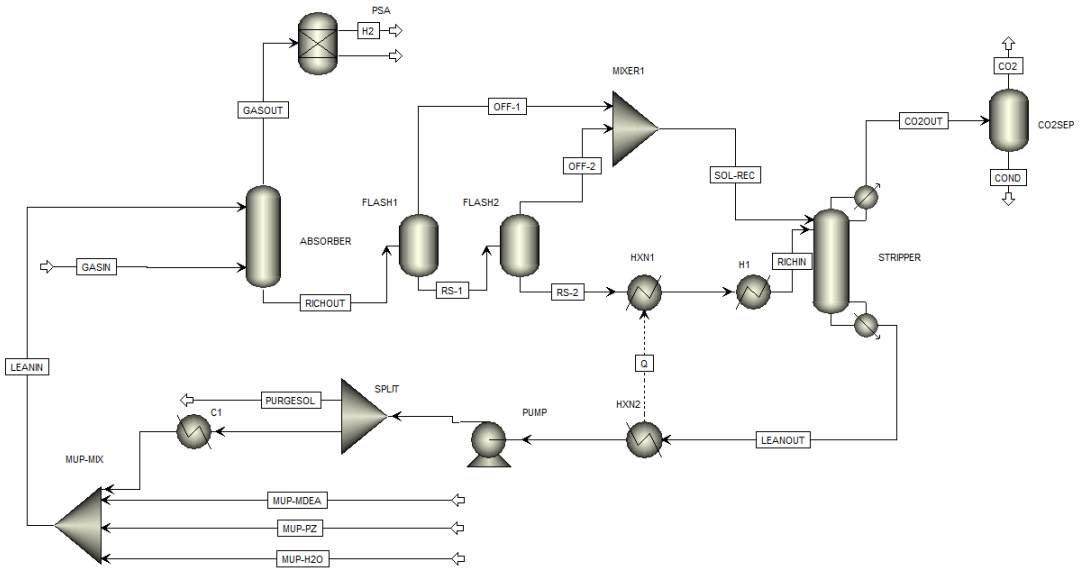

Figure 4.4: Aspen Plus flowsheet of the aMDEA recirculated model.

4.4 Parameter study

A parameter study was conducted, where the carbon capture performance was investigated when different model parameters were varied. The analysis was performed using a model without recirculation, as explained in section 4.3.3. This was to combat the issue with recirculated models not providing the possibility to change only one parameter at the time. Additionally, choosing to go with the open model immensely decreased the computational time and created significantly less problems with convergence. A base case, similar to the closed loop model was used, where the different process parameters were varied one at the time. The difference from the closed loop model was a slightly lower solvent flow rate of 80 kg/s and reboiler duty of 11.05 MW. It was altered because the open loop models slightly overestimated the carbon capture efficiency compared to the closed loop model. The base case had a carbon capture efficiency of 90.01%, hydrogen purity of 0.86, rich loading of 0.539 and lean loading of 0.041.

Parameters that were varied are summarized in Table 4.10. The liquid-to-gas ratio (L/G), is the lean solvent mass flow rate divided by the syngas mass flow rate. Stripper pressure refers to the pressure in the desorption column and the pressure of the second flash tank, while absorber pressure is the pressure level in the absorption column and the solvent and syngas inflow. The MDEA/PZ ratio refers to the ratio of the mass weight percentage of MDEA and PZ in the aqueous solution. Solvent wt% is the total weight percentage of amines in the aqueous solution, with a fixed MDEA/PZ ratio equal to that of the base case. The temperature of the stripper inflow refers to the outlet temperature of the heater placed before the stripper, and the temperature absorber inflow is the temperature of the syngas and the lean solvent entering the absorption column.

Table 4.10: Parameters varied in the parameter study including the intervals investigated.

Parameter	Base case	Interval
Liquid-to-gas ratio [-]	8	6-10
Pressure stripper [bar]	1.6	1-2.2
Pressure absorber [bar]	9	7-13
MDEA/PZ ratio [-]	9	4-49
Solvent wt% [-]	50	30-60
Temperature stripper inflow [°C]	100	89-111
Temperature absorber inflow [°C]	40	30-50

4.5 Energy minimization

Based on the parameter study, some changes to the base case model were made in order to decrease the energy consumption. The base model and the optimized model were not recirculated in this scenario. The pressure of the absorber and its inlet stream was raised to 10 bar. The solvent composition was changed to

47wt% MDEA and 3wt% PZ. With the changes implemented, an optimization was performed with the objective to minimize energy consumption while achieving a capture rate of 90%. The focus was to decrease the duty of the heat exchanger prior to the stripper column as well as the reboiler duty. The heat demand from the reboiler and the heat exchanger was calculated for different L/G ratios at different pressure levels in the stripper. The stripper pressure and L/G ratio with lowest heat demand was added to the final optimized model. A comparison of the base model and the optimized model was then made.

5
Analysis and Discussion

5.1 Parameter study

5.1.1 Solvent composition and flow

Figure 5.1 (a) show how capture rate change for different solvent compositions when the liquid to gas ratio in the absorber is varied. The inlet flow of gas is held constant at 10 kg/s, while the lean solvent flow is varied between 60 and 100 kg/s. The lean flow was set to contain 50 wt% of solvent, and each line in the graph represents set values for PZ wt%. MDEA wt% was adjusted for each scenario to maintain total solvent concentration of 50 wt%. In Figure 5.1 (b) the absorption efficiency of the absorber for each PZ wt% scenario is presented. The conditions are the same as described for Figure 5.1 (a).

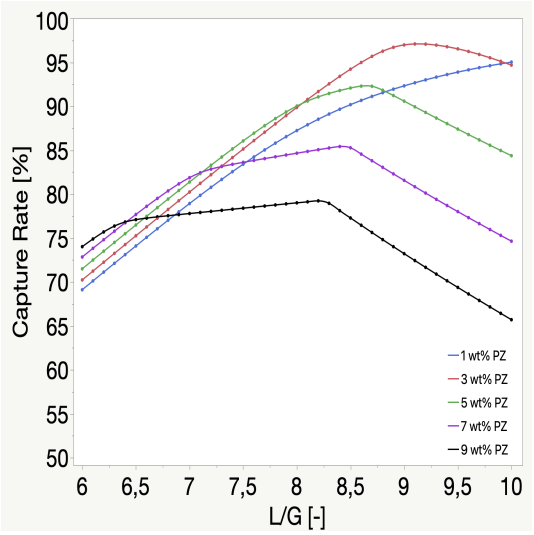

(a) Capture rates for varying liquid to gas ratio. Each line represents different wt% of PZ in the solvent. MDEA content varies accordingly to achieve a total solvent wt% of 50.

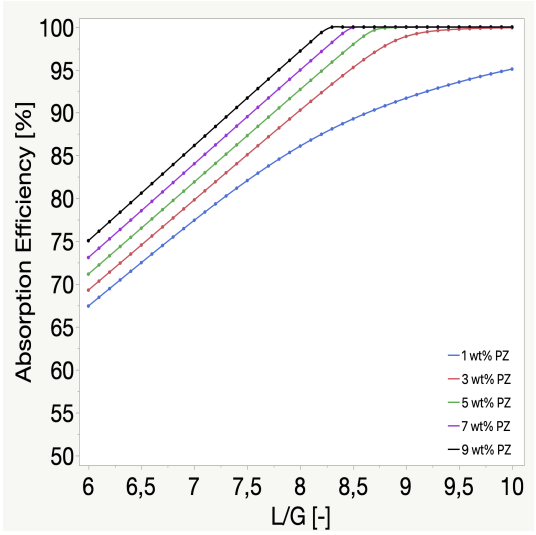

(b) Absorption efficiencies for varying liquid to gas ratio. Each line represents different wt% of PZ in the solvent. MDEA content varies accordingly to achieve a total solvent wt% of 50.

Figure 5.1: The influence of varying solvent flow rate and composition on capture rate and absorption efficiency.

In Figure 5.1 (a), it is shown that capture rates increase with increasing liquid to gas ratio, until it reaches a maximum. After this point, capture rates start to

decline. Solvent compositions with higher PZ content reaches maximum capture rates at a lower liquid-to-gas ratio, compared to solutions with less PZ. Figure 5.1 (b) shows that absorption efficiencies increases with increased liquid to gas ratios and that maximum absorption efficiencies of close to 100% are reached more rapidly with higher wt% of PZ. Comparing Figure 5.1 (a) with (b), the liquid to gas ratio where capture efficiencies reaches a maximum corresponds to when the absorption efficiency approaches 100%. Increased absorption rates as a result of higher liquid to gas ratios can be explained by the fact that more amines are present and able to react with CO_2. The higher liquid to gas ratios requires a larger reboiler duty to achieve the same stripper performance and thus maintain high capture efficiencies. Meaning that the energy demand for solvent regeneration increases with higher solvent flow rates. This corresponds to findings in literature [44]. In this case, the reboiler duty was kept constant, which is why a significant drop in capture efficiency is shown in the graph after the maximum absorption efficiency is reached. Worth to mention is that a fully recirculated system would require the reboiler duty to increase with increased L/G to obtain adequate capture efficiencies. Otherwise, CO_2 would accumulate and the values for lean loading in the input for the absorber would not match the output of the stripper which probably would cause absorption efficiencies to change. Figure 5.1 (b) shows that for the cases with higher wt% of PZ, maximum absorption is reached at lower L/G ratios. This is in line with literature findings. Studies have shown that absorption efficiency increases with higher PZ content in an aMDEA solution. The reason being that PZ have higher reaction rates and faster reaction kinetics compared to MDEA, which benefits the absorption rate [45]. Additionally, PZ has a cyclic secondary amine structure and one mole of PZ may theoretically react with two moles of CO_2 whereas MDEA only can react with one mole due to it being a tertiary amine [45]. MDEA however have a relatively low heat of reaction with CO_2, and thus requires less heat for solvent regeneration meaning a lower reboiler duty is needed to achieve decent stripper performance [45]. This may also explain why capture efficiencies are lower for the cases with higher PZ weight percentages when liquid gas ratios are high enough to achieve high absorption efficiencies. Additionally, it has been reported that for higher total solvent concentrations (more than 40 wt%), aMDEA solutions are favored by lower PZ concentrations because the PZ increases the viscosity of the solution, which increases liquid mass transfer resistance and lowers the process performance [46].

5.1.2 Pressure

5.1.2.1 Absorber pressure

Figure 5.2 (a) displays the effect of changing the pressure level in the absorption column on the capture efficiency. In Figure 5.2 (b) the effect of varying absorber pressure on CO_2 loading is presented. The pressure level is varied between 7 and 13 bars in increments of 0.5 bars.

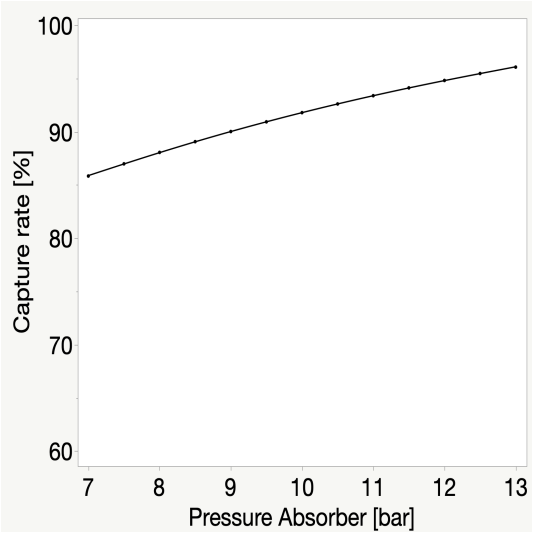

(a) Capture rate for varying pressure in the absorption column.

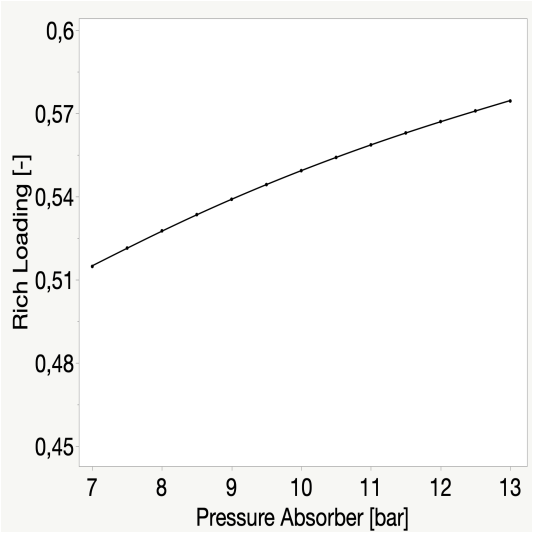

(b) Rich loading for varying pressure in the absorption column.

Figure 5.2: The influence of varying pressure in the absorber on capture rate and rich loading.

In Figures 5.2 (a) and (b) capture rate and rich loading follow a similar pattern when the absorber pressure is varied. A higher pressure in the absorber increases loading at the bottom stage, meaning more CO_2 has been absorbed into the solvent material. The higher pressure in the absorber increases the partial pressure and thereby result in a larger driving force for CO_2 absorption. A higher rich loading means that more carbon dioxide reaches the stripper, where the solvent can be regenerated and release the CO_2, which is extracted at the top of the stripper. Thereby, it benefits the stripper performance and result in higher capture efficiency. Increased capture rates due to higher pressures in the absorber is in line with literature findings [2]. It should be noted that the binary coefficients from the Aspen Plus database are only valid up to 10 bar, making the results for higher pressure levels more uncertain. In an experimental study by Khan et al. [47] it was however found that CO_2 rich loading, i.e. solubility, increased with increased pressure, thus following a similar pattern as the simulation results in this thesis. The study used an aqueous solution of MDEA, and different MDEA and PZ blends with pressure levels varying between atmospheric pressure up to 15 bar [47].

5.1.2.2 Stripper pressure

Figures 5.3 (a) and 5.3 (b) show how capture rate of the model and heat demand in the heat exchanger prior to the stripper is affected by changing the pressure in the stripper column. The pressure level was varied between 1 and 2.2 bar.

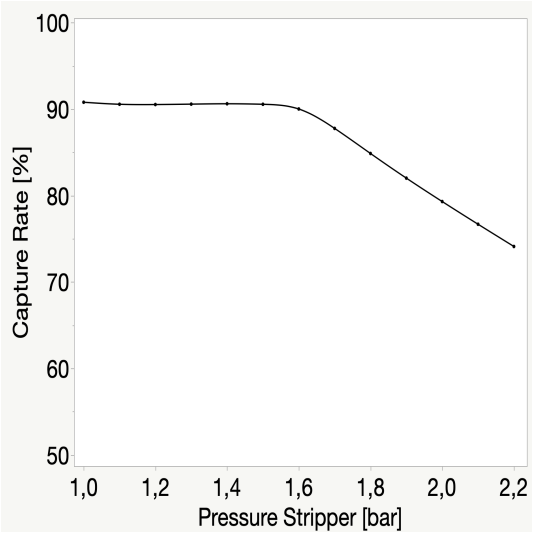

(a) Capture rate for varying pressure in the desorption column.

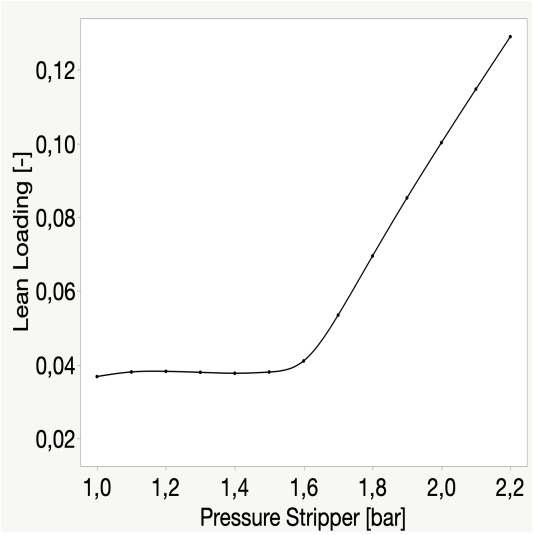

(b) Lean loading for varying pressure in the desorption column.

Figure 5.3: The influence of varying pressure in the stripper on capture rate and lean loading.

Figure 5.3 (a) shows how the process capture rate decreases with higher pressures in the stripper. This is due to the phase change from liquid to gaseous phase is favored by lower pressure. There is only a slight decrease in capture efficiency until the curve reaches a pressure level of 1.6 bar. This is due to the base case being 1.6 bar, meaning that the reboiler duty is designed for that case, which means that for lower pressure levels, the reboiler duty is overdimensioned if aiming for a capture efficiency of 90%. The reason why the capture efficiencies are not higher below 1.6 bar is that the capture efficiency is limited by the performance of the absorber. The stripper can only release the CO_2 that has been absorbed. In Figure 5.3 (b) it shows that the lean loading increases with increased pressure, meaning that for higher pressure levels, more CO_2 is left in the regenerated solvent stream. This also explains the lower capture rates for higher pressure levels, since CO_2 exits with the solvent stream in the bottom of the stripper instead of being released at the top in the CO_2 rich gas stream.

5.1.3 Temperature

5.1.3.1 Absorber feed temperature

Figure 5.4 (a) and (b) shows how capture rate and rich loading in the absorber changes, when the temperature of the syngas feed stream and lean solvent stream is varied between 30 °C and 50 °C. The two inlet streams had the same temperature for each simulation run.

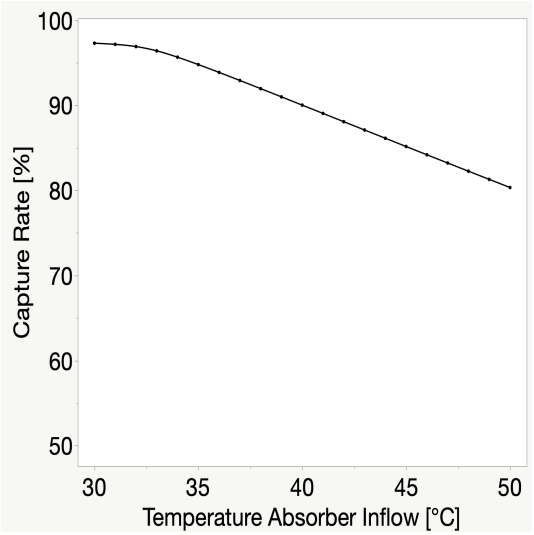

(a) Capture rate for varying temperature into the absorption column.

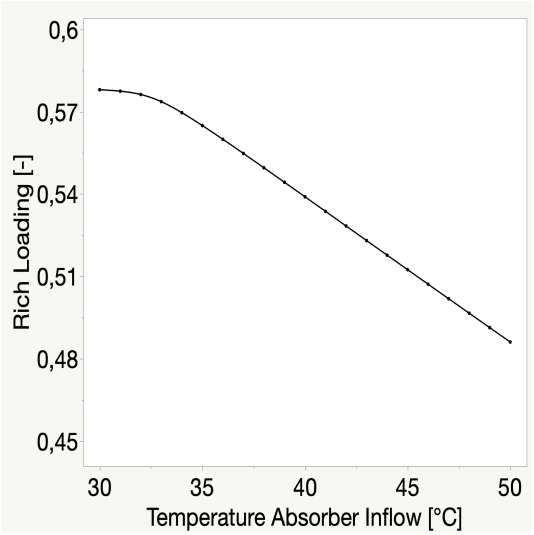

(b) Rich loading for varying temperature into the absorption column.

Figure 5.4: The influence of varying feed temperature into the absorber on capture rate and rich loading.

From Figure 5.4 (a) and (b) it is apparent that a lower temperature of the absorber feed streams result in a higher absorption of CO_2. This also gives the process a higher capture rate, since the stripper receives larger amount of CO_2 from the rich solvent. As the inlet temperature increase, the rich loading is decreased, and thus also the total capture rate of the system. Lower temperatures favors absorption, since the solubility increases with temperature. It does however have an opposite effect on the reaction rates, since higher temperatures would result in faster reactions. In this case with reactive absorption, it is likely that the reaction rates are already so high that the temperature difference does not have a significant impact on the reaction rates. Meaning that solubility has the main influence on the absorption performance, which would explain the decreasing capture rate due to higher temperatures. Lower feed temperatures however increases the demand for cooling in the process which should be weighed against the benefit of improved absorption.

5.1.3.2 Stripper feed temperature

Figure 5.5 (a) and (b) shows how capture efficiency and lean loading vary when changing stripper feed temperature. The outlet temperature of the heat exchanger previous to the stripper column was altered between 89-111 °C whereas all other process parameters were kept constant, according to the base case.

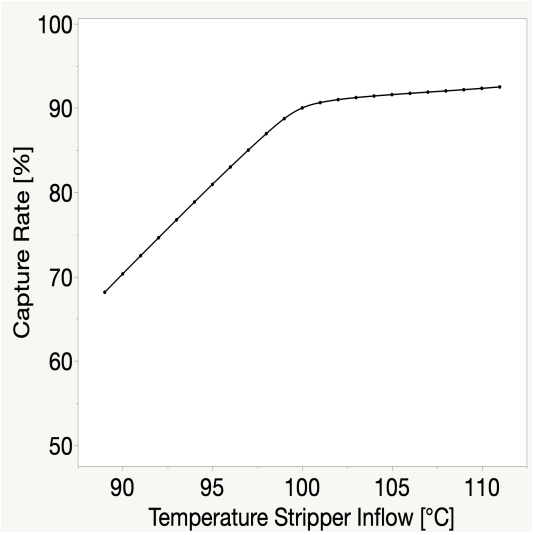

(a) Capture rate for varying temperature into the stripper column.

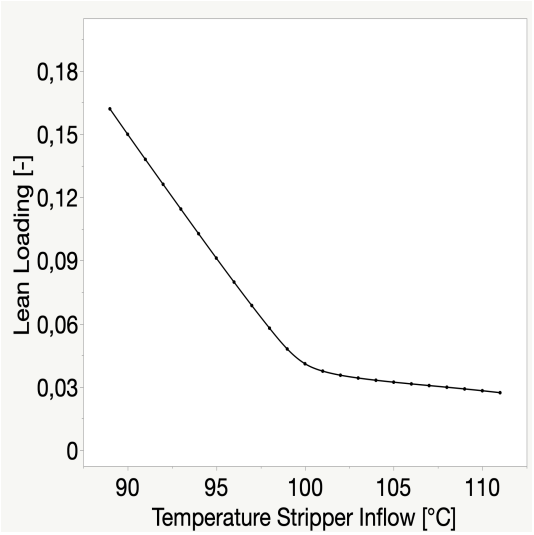

(b) Lean loading for varying temperature into the stripper column.

Figure 5.5: The influence of varying inlet temperature to the stripper column on capture rate and lean loading.

Figure 5.5 (a) shows that capture efficiency is favored by higher inlet temperature. For values below the base case (100 °C), it is apparent that the capture efficiencies have a large temperature dependency. For values above the base case, the increase is not as rapid. For those values, the slower increase may be explained by the stripper reboiler duty being overestimated if aiming for a high ($\geq$ 90%) capture rate and that the capture rate is limited by the performance of the absorber. Looking at Figure 5.5 (b), the curve shows low values for lean loading for temperatures higher than the base case, meaning that there is a low CO_2 content in the regenerated solvent, making it hard to reach higher capture rates. For the temperatures below 100 °C, there is not enough heat available to regenerate the solvent which leads to a lower capture rate. This is also shown in Figure 5.5 (b), where lean loading is higher at lower stripper inflow temperatures. It means that more CO_2 is left in the lean solvent stream. Worth mentioning is that for a temperature of 89 °C, there is no need to include an extra heat exchanger since there is sufficient heat that can be transferred in the cross heat exchanger. That would however require changing other process parameters to achieve a sufficient capture rate, for example increased reboiler duty and lower stripper pressure.

5.2 Optimization

5.2.1 Energy minimization

Figure 5.6 shows how the total heat demand in the carbon capture model changes for varying liquid-to-gas ratios. The heat demand includes the reboiler duty and the duty of the heat exchanger prior to the stripper column. The different lines represents different stripper pressures, varied between 1.6 bar and 2.2 bar.

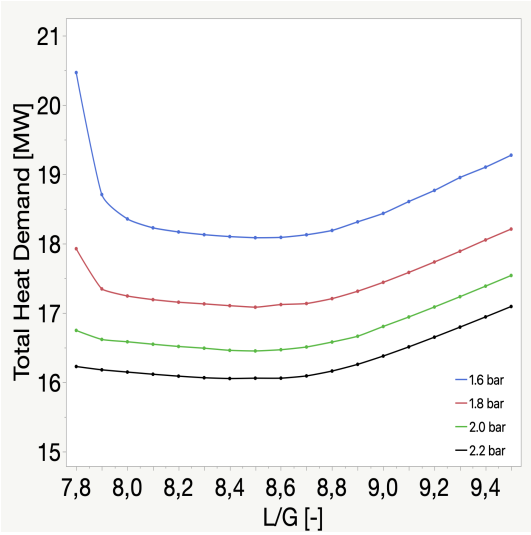

Figure 5.6: Heat demand in the carbon capture process for different liquid-to-gas ratios. Each line represents different pressure in the stripper column.

Figure 5.6 show that a higher pressure in the desorption column has a positive impact on the total heat demand for the carbon capture process. Higher pressure in the stripper gives a lower total heat demand. Each line in the graph shows that a minimum value exist for total heat demand, corresponding to a specific liquid-to-gas ratio. The lowest total heat demand found in the graph is for the case with 2.2 bar, at a liquid-to-gas ratio of 8.4. Heat demand at this point is 16.05 MW. The fuel intake for the process is planned to be 50 MW, which shows that the heat demand for the carbon capture process is significant compared to the planned energy output. This means that measures to decrease the energy consumption of the carbon capture process is important in order to achieve a cost competitive plant. An important part of these measures will be to investigate new possibilities for heat integration in the system by expanding the system boundary to include the gasification unit. For high L/G values, the total heat demand increases for all pressure scenarios. When the mass flow of solvent increases in the process, so does the heat required to increase temperature of the solvent stream, as well as reboiler duty necessary to regenerate the solvent. This explains the increased total heat demand for higher liquid-to-gas ratios.

Increasing stripper pressure will increase lean loading at the bottom of the stripper, as seen in Figure 5.3. To achieve a capture rate of 90% when stripper pressure is increased, the reboiler is therefore required to deliver more heat in order for the rich solvent to regenerate and release CO_2. As reboiler duty is increased, the temperature of the regenerated lean solvent will rise. With a higher temperature of the lean solvent stream higher, more heat can be transferred in the cross heat exchanger. This will increase the temperature of the rich solvent stream that enters the heater prior to the stripper column, decreasing the required duty of the heater. The gain from decreased demand for hot utility in the heater, is larger than the energy loss from an increased reboiler duty in terms of MW. Increasing the pressure of the stripper column will thus decrease the total heat demand of the process, as the increase

in reboiler duty is beneficial to the heat integration of the process.

5.2.2 Model comparison

In Table 5.1, the difference in process parameters and energy demand for the base model and the final optimized model are presented. The heat demand is decreased in the final optimized model, whereas the cooling demand is increased. The change in heat demand is partly a result of the optimization of L/G ratio and stripper pressure shown in figure 5.6. Moreover, the change in MDEA/PZ ratio lowers the reboiler duty due to the lower energy requirement of regeneration of MDEA compared to PZ. The increased absorber pressure also contributes by improving the absorption efficiency which result in more CO_2 entering the stripper column, making the energy requirement to capture the same amount of CO_2 less. The higher cooling duty in the final model may be explained by the higher solvent flow rate in the final model. Furthermore, the outlet temperature of the rich solvent stream from the second flash tank will be slightly higher in the final model due to the higher pressure. This means that the cross heat exchanger cannot cool the lean solvent stream as much when being restricted to a minimum temperature difference of 10 °C. It will therefore also contribute to a larger demand in the cooler. The difference in heat demand is however larger than the difference in cooling demand and if assuming a higher cost for heating utility compared to cooling utility, the cost for energy would be less in the final model. The electricity consumption in the pump is slightly increased in the final model, since it has a higher solvent flow rate and a marginally larger pressure difference. It would thus result in a somewhat higher electricity cost. Additionally, the cost for solvent is increased in the final model due to the higher L/G ratio.

Table 5.1: The difference in process parameters and energy requirement for the base model and the final optimized model.

Process conditions	Base model	Final model
Liquid-to-gas ratio [-]	8	8.4
MDEA/PZ ratio [-]	9	15.7
Pressure stripper [bar]	1.6	2.2
Pressure absorber [bar]	9	10
Tot heat demand [MW]	18.74	16.05
Specific heat demand [MJ/kgCO_2]	2.45	2.10
Tot cooling demand [MW]	10.79	11.66
Specific cooling demand [MJ/kgCO_2]	1.41	1.53

Other process parameters that may be altered to minimize the energy demand further is the total solvent wt%, the column inlet temperatures and the absorber cooling duty.

6
Conclusion

In this thesis a chemical absorption carbon capture model, constructed in Aspen Plus, has been evaluated in order to determine important design parameters and their impact on process performance. Parameters that were investigated where primarily liquid-to-gas ratio, solvent stream composition, pressure levels in the absorption and desorption columns, as well as temperatures of feed streams to absorption and desorption columns.

It was found that liquid-to-gas ratio can have a large impact on the capture rate of the process, due to a higher absorption efficiency for higher solvent flows. The composition of the solvent stream was also found to be an important design parameter, as the difference in kinetic and thermodynamic properties of PZ and MDEA creates a scenario where an optimal mix can be found in order to achieve a desired rate of carbon capture. High amounts of PZ will yield higher capture rates and absorption efficiencies for lower liquid-to-gas ratios compared to cases with low amounts of PZ in the solvent stream. This is because PZ has faster reaction rates with CO_2 than MDEA, and the fact that one mole of PZ can react with two moles CO_2 compared to MDEA that can only react with one. However, since PZ demands more heat than MDEA to be regenerated in the desorption column, a high PZ wt% could decrease the overall performance of the process when aiming for high capture rates of CO_2.

Pressure levels in the absorption and desorption column, were found to have large impacts on capture performance, as well as total heat demand of the process. Increasing the absorber pressure yields increased rich loading. This increase in amount of carbon absorbed in the solvent means that overall carbon capture rate is increased for the process, as the stripper receives increased amounts of CO_2 that can potentially be captured. The pressure in the desorption column was shown to impact the overall heat demand of the process. The higher reboiler duty required to achieve sufficient capture rates with higher stripper pressure result in increased temperature of the lean solvent stream. This allows more heat to be transferred in the cross heat exchanger and thus lowers the demand for hot utility in the heat exchanger prior to the desorption column.

The feed temperatures to the absorber and stripper was shown to affect CO_2 loading of the outlet solvent streams. The absorption column achieves higher rich loading for lower temperatures, due to increased solubility. The high value for rich loading, increases the capture rate since more CO_2 reaches the stripper. Varying the temperature of the stripper feed showed that higher capture rates can be achieved when

increasing the temperature. This may be a result of decreased solubility for higher temperatures as well as the endothermic regeneration reactions being favoured by higher temperatures.

7
Future work

7.1 Model and methodology improvements

There are opportunities for improving the methodology used for evaluation of the model conducted in this thesis, as well as opportunities for improving the model itself. The model could be further developed in order to achieve a more optimal process in terms of energy requirement and cost efficiency. It may also be improved in terms of giving a better accuracy for describing reality. Some examples of improvements are presented in this section.

The parameter study could be performed using a fully recirculated model, taking into account how the stripper performance affect the absorption. This would impact computational time and might create convergence issues. Additionally, an optimization with regards to equipment sizing could be done in order to decrease investment costs and to achieve optimal column performance. Degradation reactions for the amines could also be included in the model since degradation will have an impact on the performance of the capture unit, and will also influence the cost of solvent make up. Lastly, the model could potentially give better results if more theoretical stages in the RadFrac columns were introduced. The number of stages correspond to the number of CSTRs in series. This means that a significantly high number is required to be able to investigate if the column functions as an ideal plug-flow reactor and to get an accurate numerical solution. This will however have a large impact on convergence and computational time for the model.

7.2 Research questions

It would be interesting to do a technoeconomical investigation of the carbon capture process, comparing costs for energy, solvent and equipment to find a proper cost optimization. Furthermore, an expansion of the system boundary including the gasification unit could be done to for example evaluate opportunities for heat integration within the whole system. In our case, it is assumed that the gasification unit works under optimal conditions. Therefore it could also be interesting to perform an analysis investigating how the cost of producing hydrogen and capturing carbon is affected by different load conditions, and different feed compositions of biomass.

Bibliography

[1] European Commission. *Grant agreement for Bio-FlexGen*, 2021.

[2] P. Feron, *Absorption-Based Post-Combustion Capture of Carbon Dioxide*, pp.3-33. Duxford: Woodhead Publishing, 2016. ISBN: 9780081005156

[3] M. Aqib Chishty, K. Umeki, M. Risberg, A. Wingren, R. Gebart, *Numerical simulation of a biomass cyclone gasifier: Effects of operating conditions on gasifier performance*, Fuel Processing Technology, vol. 218, 2021. DOI: 10.1016/j.fuproc.2021.106861

[4] Aspen Technology, Inc., *Rate-Based Model of the CO_2Capture Process by Mixed PZ and MDEA Using Aspen Plus*, pp. 3-18, 2014.

[5] IPCC. *Climate Change 2013: The Physical Science Basis. Contribution of Working Group I to the Fifth Assessment Report of the Intergovernmental Panel on Climate Change*, Cambridge, United Kingdom and New York, USA: Cambridge University Press, pp. 33-115, 2013.

[6] J. Blunden, T. Boyer. *State of the Climate in 2020* Bulletin of the American Meteorological Society, vol. 102 (8), pp. Si–S475. DOI:10.1175/2021BAMSStateoftheClimate.1

[7] ESCI. *Bio-FlexGen* Available at: `https://bioflexgen.eu/guide.html` Accessed: 2022-01-26.

[8] J.P. Badeau, A. Levi. *Biomass Gasification: Chemistry, Processes and Applications*, New York: Nova Science Publishers, pp. 1-12, 2009. Available at: ProQuest Ebook Central, Accessed: 2022-04-19.

[9] J.C. Magalhaes Pires, A. L. da Cunha Goncalves. *Bioenergy with Carbon Capture and Storage: Using Natural Resources for Sustainable Development*, Academic Press, London, pp. 15-37, 2019. ISBN: 9780128162293.

[10] N. Pour, P. A. Webley, P. J. Cook. *A Sustainability Framework for Bioenergy with Carbon Capture and Storage (BECCS) Technologies* Energy Procedia, vol. 114, 2017. DOI: 10.1016/j.egypro.2017.03.1741

[11] ESCI, *Bio-FlexGen* Available at: `https://bioflexgen.eu/solutions/` Accessed: 2022-05-02

[12] Phoenix biopower, *Bio-FlexGen* Available at: `https://phoenixbiopower.com/our-technology` Accessed: 2022-05-02

[13] D. Buentello-Montoya et al.. *Performance of biochar as a catalyst for tar steam reforming: Effect of the porous structure* Applied Energy, vol. 259, 2020. DOI: 10.1016/j.apenergy.2019.114176

[14] N. Abdoulmoumine, S. Adhikari, A. Kulkarni and S. Chattanathan. *A review on biomass gasification syngas cleanup* Applied Energy, vol. 155, 2015. DOI: 10.1016/j.apenergy.2015.05.095

[15] M.A. Babatabar, M. Saidi. *Hydrogen production via integrated configuration of steam gasification process of biomass and water-gas shift reaction: Process simulation and optimization* International Journal of Energy Research, vol. 45 (13), pp. 19378-19394, 2021. DOI: 10.1002/er.7087

[16] W. Kuckshinrichs, J.K. Hake. *Carbon Capture, Storage and, Use, Technical - Economic, Environmental and Societal Perspectives* Switzerland: Springer International Publishing, 2015. ISBN: 9783319119434

[17] G. Centi, S. Perathoner et al.. *Green Carbon Dioxide: Advances in CO2 Utilization*, John Wiley and Sons, Inc, 2014, Available at: `https://ebookcentral.proquest.com/lib/chalmers/reader.action?docID=1598287`, Accessed: 2022-xx-xx.

[18] Z.H. Ban, L.K. Keong, A.M. Shariff. *Physical Absorption of CO_2 Capture: A Review*, Advanced Materials Research, vol. 917, pp. 134–143, 2014. DOI: 10.4028/www.scientific.net/AMR.917.134

[19] T. N.Borhani, S. Babamohammadi, N. Khallaghi, Z. Zhang. *Mixture of piperazine and potassium carbonate to absorb CO_2 in the packed column: Modelling study*, Fuel, vol. 308, 2022. DOI: 10.1016/j.fuel.2021.122033

[20] T. N.Borhani, M. Wang. *Role of solvents in CO2 capture processes: The review of selection and design methods*, Renewable and Sustainable Energy Reviews, vol. 114, 2019. DOI: 10.1016/j.rser.2019.109299

[21] M. Imran, U. Ali, A. Hasnain. *Impact of blends of aqueous amines on absorber intercooling for post combustion CO_2 capture system*, Energy & Environment, vol. 32 (5), pp. 921-944, 2021. DOI: 10.1177/0958305X20982835

[22] B. Aghel, S. Sahraie, E. Heidaryan, K. Varmira. *Experimental study of carbon dioxide absorption by mixed aqueous solutions of methyl diethanolamine (MDEA) and piperazine (PZ) in a microreactor*, Process Safety and Environmental Protection, vol. 131, 2019. DOI: 10.1016/j.psep.2019.09.008

[23] S.M. Hosseini-Ardali, M. Hazrati-Kalibibaki, M. Fattahi, and F. Lezsovits. *Multi-objective optimization of post combustion CO_2 capture using methyldiethanolamine (MDEA) and piperazine (PZ) bi-solvent*, Energy, vol. 211, 2020. DOI: 10.1016/j.energy.2020.119035

[24] A.J. Reynolds, T.V. Verheyen, E. Meuleman. *Absorption-Based Post-combustion Capture of Carbon Dioxide*, Editor(s): P. Feron, pp.399-423. Duxford: Woodhead Publishing, 2016. ISBN: 9780081005156

[25] C. Gouedard, D. Picq, F. Launay, P.-L. Carrette. *Amine degradation in CO2 capture. I. A review*, International Journal of Greenhouse Gas Control, vol. 10, pp. 244-270, 2012. DOI: 10.1016/j.ijggc.2012.06.015

[26] S. A. Mazari, A. S. Brahim, J. M. Badrul, I. M. Saeed, S. Nizamuddin. *An overview of solvent management and emissions of amine-based CO2 capture technology*, International Journal of Greenhouse Gas Control, vol. 34, pp. 129-140, 2015. DOI: 10.1016/j.ijggc.2014.12.017

[27] M. Luberti, H. Ahn. *Review of Polybed pressure swing adsorption for hydrogen purification*, International Journal of Hydrogen Energy, vol. 47, pp. 10911-10933, 2022. DOI: 10.1016/j.ijhydene.2022.01.147

[28] A. Abbas Obaid, S. Farokhi, A. Bayat. *A novel process simulation model for hydrogen production via reforming of biomass gasification tar*, Interna-

tional Journal of Hydrogen Energy, vol. 47, no. 2, pp. 772-781, 2022. DOI: 10.1016/j.ijhydene.2021.10.055

[29] , IEA, *The Future of Hydrogen*, 2019. Available at: `https://www.iea.org/reports/the-future-of-hydrogen` Accessed: 2022-05-03

[30] D.-Y. Peng, D. B. Robinson, *A New Two-Constant Equation-of-state*, Industrial Engineering Chemistry Fundamentals, vol. 15, pp. 59–64, 1976.

[31] D.M. Austgen, G.T. Rochelle, C.C. Chen. *Model of Vapor-Liquid Equilibria for Aqueous Acid Gas-Alkanolamine Systems. 2. Representation of H_2S and CO_2 Solubility in Aqueous MDEA and CO_2 Solubility in Aqueous Mixtures of MDEA with MEA and DEA*, Industrial Engineering Chemistry Research, vol. 30, pp. 543-555, 1991. DOI: 10.1021/ie00051a016

[32] S. Bishnoi, G. Rochelle. *Absorbtion of Carbon Dioxide into Aqueous Piperazine: Reaction Kinetics, Mass Transfer and Solubility*, Chemical engineering Science, vol. 55, pp. 5531-5543, 2000. DOI: 10.1016/S0009-2509(00)00182-2

[33] M.D. Hilliard. *A Predictive Thermodynamic Model for an Aqueous Blend of Potassium Carbonate, Piperazine, and Monoethanolamine for Carbon Dioxide Capture from Flue Gas*, Ph.D. Dissertation, University of Texas at Austin, 2008.

[34] O. Redlich, J.N.S. Kwong. *On the Thermodynamics of Solutions V. An Equation-of-state Fugacities of Gaseous Solutions*, Chemical Reviews, vol. 44, pp. 223 – 244, 1949.

[35] C. Madeddu, M. Errico, R. Baratti. *CO2 Capture by Reactive Absorption-Stripping Modeling, Analysis and Design*, 1st ed. Springer International Publishing, 2019 . Available at: `https://search.ebscohost.com/login.aspx?direct=true&db=cat07472a&AN=clec.SPRINGERLINK9783030045791&site=eds-live&scope=site` Accessed: 2022-04-20

[36] A. I. Papadopoulos, P. Seferlis. *Process systems and materials for CO_2 capture : modelling, design, control and integration*, Wiley, pp. 283-310, 2017. DOI: 10.1002/9781119106418

[37] W. K. Lewis, W. G. Whitman. *Principles of Gas Absorption* Industrial Engineering Chemistry, vol. 16, pp. 1215-1220, 1924. DOI: 10.1021/ie50180a002

[38] J. R. Welty. *Fundamentals of Momentum, Heat and Mass Transfer*. 6th edition, International student version, John Wiley Son, pp. 533-538, 2015. ISBN: 9781118808870

[39] M. Errico, C. Madeddu, D. Pinna, R. Baratti. *Model calibration for the carbon dioxide-amine absorption system*, Applied Energy, vol. 183, pp. 958-968, 2016. DOI: 10.1016/j.apenergy.2016.09.036

[40] A. Hemmati, H. Rashidi. *Mass transfer investigation and operational sensitivity analysis of amine-based industrial CO_2 capture plant*, Chinese Journal of Chemical Engineering, vol. 27, pp. 534-543, 2019. DOI: 10.1016/j.cjche.2018.07.014

[41] J.L. Bravo, J.A. Rocha, J.R. Fair. *Mass transfer in gauze packings*, Hydrocarbon Processing, vol. 91, 1985.

[42] R. Taylor, R. Krishna. *Multicomponent Mass Transfer*, New York: Wiley, 1993. ISBN: 0471574171

[43] R. Billet, M. Schultes. *Predicting Mass Transfer in Packed Columns*, Chemical Engineering Technology, vol 16, 1993. DOI: 10.1002/ceat.270160102

[44] M. Zhang, Y. Guo. *Optimization of Carbon Capture Process Using Aqueous Ammonia with Rate-based Simulation Method*, Energy Procedia, vol 114, 2017. DOI: 10.1016/j.egypro.2017.03.1270

[45] A. A. Khan, GN. Halder, A.K. Saha. *Experimental investigation on efficient carbon dioxide capture using piperazine (PZ) activated aqueous methyldiethanolamine (MDEA) solution in a packed column*, International Journal of Greenhouse Gas Control, vol 64, 2017. DOI: 10.1016/j.ijggc.2017.07.016

[46] S. Saleh, A. Razali, R. Hanafiah, A. Tamidi and Z. P. Chan. *Optimization of MDEA-PZ Ratio and Concentration for CO_2 Removal in Semi-Lean Membrane Contactor Process*, E3S Web Conference, vol 287, 2021. DOI: 10.1051/e3sconf/202128703009

[47] S. N. Khan et al., *High-pressure absorption study of CO_2 in aqueous N-methyldiethanolamine (MDEA) and MDEA-piperazine (PZ)-1-butyl-3-methylimidazolium trifluoromethanesulfonate [bmim][OTf] hybrid solvents*, Journal of Molecular Liquids, vol 249, pp. 1236-1244, 2018. DOI: 10.1016/j.molliq.2017.11.145

DEPARTMENT OF SPACE, EARTH AND ENVIRONMENT
CHALMERS UNIVERSITY OF TECHNOLOGY
Gothenburg, Sweden
www.chalmers.se

CHALMERS
UNIVERSITY OF TECHNOLOGY